Lifelong F&V intake attenuates liver cancer in aged mice concomitant with gut microbiome and sphingolipidome remodeling

by

Edwin F. Ortega, M.S.

Biochemical and Molecular Nutrition Program
Friedman School of Nutrition Science and Policy
Tufts University

A dissertation submitted for the degree of Doctor of Philosophy
April 2023

Thesis Advisor/Chair:
Simin N. Meydani, D.V.M., Ph.D.
Emeritus Professor, and Research Professor of Nutrition
Friedman School of Nutrition Science and Policy
Faculty member, Graduate School of Biomedical Sciences
Tufts University
simin.meydani@tufts.edu

Thesis Committee Members:
Dayong Wu, M.D., Ph.D
Associate Professor
Friedman School of Nutrition Science and Policy
dayong.wu@tufts.edu

Alexander Panda, M.D., Ph.D., M.P.H.
Scientist II
Nutrition Immunology Laboratory
Jean Mayer USDA Human Nutrition Research Center on Aging at Tufts University
alexander.panda@tufts.edu

Jimmy Crott, Ph.D.
Associate Professor
Pathology & Laboratory Medicine
Boston University Chobanian & Avedisian School of Medicine
jcrott@bu.edu

Abstract

Aging is a natural progressive process that impairs host fitness and increases the risk for age-related disease such as cancer, cardiovascular disease, and neurodegeneration. Age-related diseases account for 23% of the total global burden of disease and the proportion of the burden is highest in high-income countries like the U.S. Since the number of older individuals is expected to increase, identifying mechanisms to mitigate age-related disease is critical. Epidemiological studies link high intake of fruits and vegetables (F&V) to increased life- and health-span. However, how F&V intake attenuates age-related disorders and disease risk is unknown. One potential mechanism by which F&V may delay age-related disease risk is through its effects on the gut microbiome. A growing body of evidence links the gut microbiome to host health and disease risk, as well as frailty. Thus, manipulation of the gut microbiome via F&V supplementation may be an attractive prevention strategy to promote healthy aging. We conducted a longitudinal mouse study in which mice were fed a low-fat (LF) or high-fat (HF) diet with or without F&V until one group reached a median lifespan of 50%. We observed a significant 50% increase in median lifespan, a 23% reduction in liver cancer incidence in mice fed a HF diet supplemented with F&V in comparison to mice fed a HF diet alone (HF-C). A non-significant (11%) increase in median lifespan and a significant decrease in the levels of systemic markers of inflammation was observed in mice fed a LF diet supplemented with F&V in comparison to mice fed a LF diet alone (LF-C). The goal of this thesis project was to characterize the gut microbiome in mice fed HF or LF diet in aged mice as well as their F&V supplemented counterparts. Further, we sought to link diet- and age-associated microbiota changes to liver cancer, systemic inflammation, a hallmark of aging, and putative biomarkers of aging and disease, such as sphingolipids. We report that lifelong intake of F&V is linked to a unique microbiome composition, particularly an enrichment of potent short-chain fatty acid producing bacteria, such as *ASF356* and *Lachnospiraceae NK4A136*. F&V attenuated the age- and obesogenic-associated increase in harmful bacteria, such as *Streptococcus*. Lean mice supplemented with F&V maintained levels of health-associated *Bifidobacterium,* which was associated with a reduced risk of liver cancer. The bacteria belonging to the *Romboutsia* and *[Ruminococcus] torques group* genera were positively associated with liver cancer*,* both of which were increased in the HF-C in comparison to mice fed HF-diet with F&V supplementation. Mice supplemented with F&V also had an increased Firmicutes/Bacteroidetes ratio at the end of the study in comparison to their non-F&V

supplemented counterparts. Multi-omic data integration using sparse projection of latent structure discriminant analysis (sPLS-DA) revealed strong positive associations between circulating cytokine, interleukin (IL)-10, and circulating levels of sphingomyelins (SM), as well as microbiota. The features that were best at discriminating liver cancer status, such as IL-10, total SM, or *Romboutsia*, were predominantly present or higher in mice fed HF diet without F&V supplementation. Towards determining the potential mechanisms and origins of the observed changes in sphingolipids and Il-10, and their link to the gut microbiome, we interrogated the expression of genes involved in sphingolipid metabolism and IL-10 in the liver, where the cancer was present, and in the colon, the tissue in immediate vicinity to the gut microbiome. In the liver, HF-C fed mice increased their expression levels of IL-10 and acid ceramidase and reduced expression of acid sphingomyelinase in comparison to LF-C. In the colon, we found that IL-10 expression was modestly higher in the liver tissue of HF-C in comparison to LF-C mice. Increased expression of IL-10Ra was also observed in the liver of HF-C mice in comparison to both LF-C or HF-FV. Interestingly, in the colon, a 4-fold increase in IL-10 expression was observed in HF-C fed in comparison to LF-C. These results may be leveraged to inform future aging obesity studies and/or our own future mechanistic studies into the effects of lifelong F&V supplementation. Taken together, this thesis demonstrates that: 1) the gut microbiome is responsive to F&V supplementation as demonstrated by the unique microbiome compositions and specific genera linked to F&V intake, 2) the presence of liver cancer is associated to a unique set of sphingolipids, cytokine, and microbiota, and the variables best able to discriminate presence of liver cancer were predominantly enriched or present in HF-C mice, 3) HF-diet fed mice were associated with specific gene signatures that may promote a pro-survival/tumorigenic and immunosuppressive environment which may play a role in the etiology of HF-diet induced liver cancer. On the other hand, F&V was associated with a reduction or absence of many of the features associated with presence of liver cancer, which, in combination, may reduce the risk of liver cancer despite being fed HF-diet.

Table of Contents

List of Tables and Figures

SFig 2: Firmicutes/Bacteroidetes ratio calculated from relative abundance and composition bar plots (phylum level) reveal increased levels of Firmicutes and reduced Verrucomicrobiota with F&V supplementation.

SFig 3: F&V has minor impact on circulating levels of Hex-Cer and no significant differences in liver levels of Hex-Cer.

SFig 4: Sparse projection latent structure discriminant analysis selected variables and respective weights for the four blocks in component 1 and 2 that can best discriminate Liver cancer status

SFig 5: SFig 5: Receiver operating characteristic curves for each ‘omic’ block using component 1 and 2

Introduction: General Statement of the Problem Studied and Its Significance

Advances in medicine and implementation of public health policies have led to a doubling of life expectancy since 1900.[1] While it is still up to debate whether the human lifespan is finite,[2] the average lifespan is expected to continue to increase.[1] However, and perhaps more importantly, an increase in the human health span, similar to that observed in lifespan, has lagged.[3] This is largely due to the fact that advanced age increases the risk of developing chronic diseases, such as cancer, insulin resistance, and cardiovascular disease. The rate of aging is dependent on an individual's inherent genetic potential as well as lifestyle and environmental factors, the latter which can accelerate the aging process, but which can be modified.[4]

Epidemiological evidence links lifestyle and dietary factors, such as exercise and intake of fruits and vegetables (F&V), to increases in not just median lifespan, but health span as well.[5,6] Furthermore, recent lines of evidence link both lifestyle and dietary factors as determinants of gut microbiome composition and function, and in turn, link its composition and function to host health and disease risk[7] as well as frailty.[8] However, a critical problem shared by epidemiological and human aging studies is that they are cross-sectional, making it difficult to conclude causality.

Despite their limitations, cross-sectional studies in older adults have demonstrated that F&V intake as well as other dietary food groups, i.e. fermented foods, are associated with distinct microbiome communities such as an enrichment of short-chain fatty acid-producing bacteria.[9] Microbiome compositions can separate populations of older adults into distinct dietary clusters, those who consumed more F&V versus those with more red meat.[9] Further, the unique compositions are associated with environmental factors in older individuals, such as living in a senior home versus a community.[9] Similarly, studies in mice have demonstrated that prebiotics or polyphenols, both of which are present in appreciable amounts in F&V, can promote enrichment and loss of specific microbiota, which in turn can be linked to biomarkers of health and disease.[10] It follows that lifelong F&V intake could be leveraged to promote the establishment and maintenance of a specific and favorable microbiome, which in turn may positively contribute to long-term host fitness.

Testing of these linkages is a worthy undertaking as it may identify a practical dietary intervention that can promote enactment of public health recommendations or behavioral changes in individuals to promote healthy aging. If true, lifelong F&V intake can reduce morbidity in later life and disease burden on the healthcare system, which is of particular importance given the expected increase in the number of older individuals with 1 or more chronic diseases.

Statement of Hypothesis to Be Tested

The central hypothesis of this thesis is to test if lifelong high intake of F&V would result in a microbiome with distinct composition, and if it was favorably associated with the health-span outcomes, such as liver cancer, and age-related biological markers, such as systemic inflammation, and sphingolipids in a longitudinal study designed to determine the life-long impact of high F&V intake on health span and lifespan. The specific aims of this thesis were as follow:

Specific Aims

Aim I: To determine if long-term F&V supplementation alters the community composition of the gut microbes in aged obese and non-obese mice, and which specific features of the gut microbiome are different.

Hypothesis I: We hypothesize that age, diet (high- vs low-fat), and F&V supplementation would affect the general composition of the gut microbiome, as assessed by β-diversity. Age has previously been linked to increasingly “personalized” microbiomes; therefore, we expect that intra-individual variability to increase with age. At a more granular level, we expect there to be specific diet- and age-driven changes in the genera that make up the microbiome. The specific changes we expect are that F&V intake will attenuate age- and HF-diet-associated enrichment of potentially harmful bacteria such as those belonging to the *Streptococcus* and *Enterococcus* genera, while maintaining the *Firmicutes/Bacteroidetes* ratio, which is typically decreased with age.

Aim II: To determine how diet- and/or age-associated changes in the microbiome are associated with liver cancer, and age-related biological markers such as systemic inflammation, and sphingolipid profile.

Hypothesis II: We hypothesize that HF-diet induced changes in the microbiome will be positively associated with liver cancer, levels of systemic pro-inflammatory cytokines, and certain sphingolipid species. Further, we expect that specific genera will be enriched with F&V supplementation and will be negatively associated with liver cancer, levels of systemic pro-inflammatory cytokines, and certain sphingolipid species.

Aim III: To elucidate the potential mechanisms underlying the association between lifelong F&V supplementation-induced changes in the microbiome, inflammatory markers, and sphingolipid profile and the reduction in liver cancer.

Hypothesis III: Both advanced age and obesogenic diet have been associated with impairments in gut barrier integrity, alterations in microbiome composition, metabolic derangements (i.e. impaired glucose metabolism), and increased systemic inflammation. In obesity, Western- or high-fat-diets have been demonstrated to induce microbiome dysbiosis and impair barrier integrity. Impaired barrier integrity permits the translocation of pro-inflammatory microbial molecules (e.g. LPS) which promotes a proinflammatory environment. Systemic low-grade inflammation can alter metabolic processes, such as glucose homeostasis. In studies of aging and obesity, the increased risk of liver disease associated with advanced age and obesity is suggested to be mediated by loss of barrier integrity and bacterial translocation. Given the strong impact of lifelong F&V intake on liver cancer[11] and the effect of short-term F&V on fatty liver,[12] we will compare the expression of genes linked to gut barrier integrity, colonic inflammation, as well as the levels of short-chain fatty acids (SCFA's) across the different groups. SCFA's, arising from the fermentation of F&V, have been demonstrated to contribute to the regulation of gut barrier integrity and inflammation.

Review of the Literature

General introduction to emerging problem

Aging is a natural progressive process that reduces human fitness and shortens human lifespan. It is generally accepted that a time-dependent accumulation of cellular damage is the general cause of aging.[13] Age-related cellular damage includes genomic instability, alterations in cellular communication, stem cell exhaustion, cellular senescence, mitochondrial dysfunction, loss of proteostasis, telomere attrition, deregulation of nutrient sensing mechanisms, and epigenetic alterations.[13] Further, the causes of aging can be separated out into two types, primary and secondary. Primary aging is natural and inherent to an individual and is typically not attributed to a specific cause. However, secondary aging is attributed to a specific cause, such as lifestyle and dietary habits. These habits, such as lack of exercise, smoking, poor diet, can accelerate the aging process, but importantly, are also modifiable.[4] In the U.S., and globally, the aged population continues to grow,[1] and will have direct impacts on our society, healthcare system, and economy.[14] While great strides have been made in medicine and public health policy to extend the human lifespan, similar advancements in health span have not been observed. This has resulted in a population with multiple comorbidities, which often arise from poor lifestyle and dietary habits,[15] and which may accelerate the aging process itself.[16] Importantly, lifestyle and dietary habits are modifiable, and therefore may be leveraged to mitigate aging.

Microbiome, fiber, and polyphenolics

Epidemiological evidence links lifestyle and dietary factors, such as exercise and intake of fruits and vegetables (F&V), to increased median lifespan and healthspan.[5,6] Recent lines of evidence link both lifestyle and dietary factors as determinants of gut microbiome composition and function, which in turn, is associated with health, disease risk,[7] and frailty.[8] It is well accepted that diet and its components can shape the composition of the microbiome.[17,18] Changes in features of the microbiome have been observed in response to pre- and probiotic[19] as well as polyphenol supplementation,[20] and caloric restriction,[21] among others.

Whereas probiotic substances directly provide the live microorganisms that confer health benefits, prebiotics, such as fiber, contain the substrate that is utilized by those health-promoting microorganisms but contain no live microbes.[19] In the large intestine gut

bacteria can ferment fiber to form many end products such as organic acids and gasses. Some of the byproducts of bacterial metabolism, such as short chain fatty acids (SCFA), can be readily absorbed.[22] Members of the Firmicutes phylum tend to produce butyrate, while members of the Bacteroidetes phylum tend to produce acetate and propionate.[23] Butyrate is the preferential metabolic fuel for gut epithelial cells,[24,25] but additional biological properties have been assigned to SCFAs. Butyrate, which has been demonstrated to have immunomodulatory properties due to it inhibition of nuclear factor kappa-light (NF-KB).[26] A mixture of SCFA-producing *Clostridia* strains, belonging to the Firmicutes phylum, have been demonstrated to enhance T-regulatory (T-reg) abundance and interleukin (IL)-10 production.[27] Interestingly, exposure to this mixture of Clostridia strains was associated with a rich TGF-β1 environment. Microbiome-derived butyrate has been demonstrated to promote the differentiation of colonic T-reg cells,[28] via induction to histone H3 acetylation in the promoter regions of the Foxp3 locus. Linking the increased differentiation of T-regs to microbial-derived butyrate, one group demonstrated that bacterial lipopolysaccharide (LPS) and peptidoglycan from *Clostridium butyricum* induced the production of tumor growth factor (TGF)-β1 from lamina propria dendritic cells via Toll-like receptor (TLR)-2 and -4 signaling.[29] A histone deacetylase (HDAC)-mediated mechanism has been described for lamina propria macrophages. Macrophages treated with butyrate have reduced production of LPS-mediated inflammatory mediators.[30] Thus, SCFA's, particularly butyrate, have the potential to be anti-inflammatory in the colon.

In addition to the effects of SCFA's on HDAC's, SCFAs can signal via G-protein-coupled receptor (GPR)-43. GPR-43, which is highly expressed in colon epithelial and immune cells, is necessary for the appropriate regulation of immune and inflammatory responses.[31] Similarly, SCFAs can enhance antibody production via GPR43 signaling.[32] and promote the expression of tight junction genes in intestinal epithelial cells,[33,34] which may strengthen the barrier to prevent bacterial translocation.

In addition to their immunomodulatory properties, SCFAs binding to GPR-43 on glucagon-like peptide (GLP)-1 secreting L cells has been demonstrated to stimulate the release of GLP-1, a gut hormone known to control insulin release and appetite.[35] Although butyrate has received much of the attention, both acetate and propionate are also readily absorbed. Acetate is able to cross the blood–brain barrier and has a direct

appetite-suppressing role in the central nervous system.[36] Propionate is the second most abundant SCFA in the portal circulation after acetate.[37] In humans, rectal administration of SCFAs to individuals who are obese was positively associated with increased fasting lipid oxidation and resting energy expenditure; changes in these parameters were positively correlated with plasma levels of acetate.[38] In a separate study, acute oral supplementation with propionate was associated with increased resting energy expenditure.[39] In mouse adipocytes, propionate increased leptin levels, via GPR-41 signaling, which decreased energy intake.[40] Together, these observations suggest that fiber and the corresponding products of bacterial fermentation, SCFA's, have potent effects on host metabolism.

Phytochemicals are found in appreciable concentrations in F&V.[41] However, owing to their chemical structure, phytochemicals are poorly absorbed in the small intestine and therefore become highly concentrated in the large intestine.[42] Polyphenolic compounds (i.e. alkyl-resorcinol) in whole foods have been demonstrated to have modest effect on immune and inflammatory markers in humans.[43] Similarly, a proanthocyanidin-rich cranberry extract has been associated with favorable changes in mucin production, gut permeability, glucose intolerance, inflammation, and biomarkers of adipose tissue and liver health.[44] A study investigating the effects of red wine polyphenols demonstrated that in the participants with metabolic syndrome, red wine polyphenol intake was associated with increases in a number of beneficial taxa such as *Bifidobacterium*, *Lactobacillus*, and butyrate-producing bacteria such as *Faecalibacterium prausnitzii* and *Roseburia*.[10] Further they demonstrated that intake of red wine polyphenols was associated with a reduction of potentially harmful bacteria such as *E. coli* and *Enterobacter*, both belonging to the *Enterobacteriaceae* family. However, unlike fiber, polyphenols and their effect on the microbiome and vice versa are underexplored. Further research is required to determine the utility of polyphenols in modulating the gut microbiome.

Obesity and the microbiome

Given the proximity of the gut microbiome to the gastrointestinal tract (GI), several studies have linked alterations in the gut microbiota to GI diseases such as inflammatory bowel disease,[45,46] irritable bowel syndrome,[47] and various forms of colitis.[48] However,

the gut microbiome has also been linked to extraintestinal diseases such as the regulation of body weight,[49] diabetes,[50] neurological[51] and liver disease.[52]

The potential role the gut microbiota could play in mediating chronic disease, i.e. metabolic syndrome, was demonstrated by Cani et al.[53] Bacterial-derived LPS was demonstrated to initiate metabolic disorders such as diabetes and obesity. Gordon et al linked the microbiome to body weight by demonstrating that transfer of normal microbiota to a germ-free (GF) mouse could produce a 60% increase in body fat content, fasting glucose, and insulin resistance.[49] The increase in body fat was linked to increased energy extraction from food (via SCFA's) as well as modulating liver fatty acid deposition. Subsequent studies by Gordon's group demonstrated that obesity was associated with a shift away from Bacteroidetes and an increase in Firmicutes.[54] The Firmicutes phylum is associated with increased butyrate production, which has anti-inflammatory and gut barrier integrity promoting properties, yet, obesity is associated with systemic low-grade inflammation and "leaky gut." It is posited that the acute increase in Firmicutes may be a protective adaptation, that is, SCFA's can acutely dampen inflammation and promote barrier integrity at the slight cost of increasing caloric intake. Further research is required to determine what role SCFAs play in the etiology or pathogenesis of obesity.

In obese individuals a concomitant increase in potentially harmful inflammation-inducing bacteria has been reported. Both human and animal studies have linked *Staphylococcus*, *Streptococcus*, *Enterobacteriaceae*, *Enterobacter*, and *E. Coli* to obesity.[55–57] Given that obesity and other metabolic disorders are associated with systemic low-grade inflammation,[57] which may be mediated by impaired gut barrier integrity, increased abundance of these bacteria may also contribute to obesity's associated pathologies, such as low-grade systemic inflammation.

Reductions in *Bifidobacterium* have been observed in obese children.[58] *Bifidobacterium* was shown to protect against obesity in animal models[56,59] via the reduction of endotoxin, which in turn was correlated with reduced inflammatory tone and improved glucose metabolism. In humans, 12-weeks of *Bifidobacterium longum* supplementation improved fasting blood glucose levels; however no effect on BMI was observed.[60] Importantly, acetate produced by *Bifidobacterium* can promote the growth of butyrate

producing bacteria,[61] indicating potential interactions between different bacteria. Together, the microbiota and their metabolites could affect whole body energy metabolism to protect or predispose individuals to obesity.

Liver disease and the microbiome

Along with the rapid increase in obesity, a concomitant increase in the prevalence of alcoholic fatty liver disease (NAFLD) has occurred.[62] NAFLD is characterized by an excessive accumulation of intrahepatic fat (steatosis) which can progress to nonalcoholic steatohepatitis (NASH). NASH, unlike NAFLD, is irreversible and can progress to fibrosis, cirrhosis, or cancer.[63] NAFLD's high prevalence projects it to become the leading contributor to the development of liver cancer.[64] Importantly, patients with liver disease are often also obese, making it difficult to disentangle microbial signatures associated with liver disease vs obesity.

In humans, NAFLD is positively associated with an increased prevalence of *Proteobacteria*, particularly the *Enterobacteriaceae* family.[65] On the other hand, a reduction in the abundance of the *Prevotella, Dorea, Coprococcus, Eubacterium*, and *Faecalibacterium* genera was observed. *Prevotella* are known SCFA producers and *Faecalibacterium* are purported to have anti-inflammatory properties.[66,67] Increases in the *Proteobacteria* phylum and *Enterobacteriaceae* family and decreases in *Faecalibacterium* and *Coprococcus* have been reported in patients with NASH.[65] A sharp reduction in *Faecalibacterium prausnitzii* is also observed in patients with cirrhosis.[68]

Fecal microbiota transplant (FMT) studies demonstrated that FMT from weight-matched obese mice with or without steatosis to GF mice can recapitulate some of the features of NAFLD.[69] FMT studies using humanized mice demonstrated that FMT from humans with NASH to GF mice was associated with transmission of hepatic steatosis and inflammation, which could be aggravated with an obesogenic diet.[70] Interestingly, the abundance of *Streptococcaceae* was the highest in HF-fed mice who received FMT from participants with NASH. A study in obese women demonstrated that patients with steatosis had reduced microbial gene richness and increased potential to process dietary lipids and synthesize endotoxin.[71] Additionally, the gut microbiome can regulate bile acid metabolism by modifying primary bile acids and converting them to secondary

bile acids, which can affect FXR signaling in the ileum to inhibit bile acid synthesis in the liver.[72] Reduction in the synthesis of bile acids has been associated with advanced cirrhosis concomitant with higher abundances of *Enterobacteriaceae* and lower abundances of *Lachnospiraceae* and *Ruminococcaceae*.[73]

Attempts to modulate or treat liver disease by targeting the microbiome using probiotics have had limited success. Eight-week supplementation with oligofructose, a fermentable fiber, in individuals with NASH was shown to improve liver function as determined by a reduction in AST levels, and a modest, but statistically insignificant drop in ALT activity.[74] However, no effect on lipid levels was observed, despite previous evidence linking propanoic acid to inhibition of fatty acid synthesis in rat hepatocytes.[75] The lack of an effect reported in this study could be due to its relatively short exposure period. In a 24-week study, NASH patients receiving a probiotic containing *Bifidobacterium longum* in combination with a prebiotic and lifestyle modifications, was demonstrated to reduce AST, LDL, CRP, TNF-α, HOMA-IR, serum endotoxin, and steatosis, in comparison to patients receiving only lifestyle modification.[76]

Ongoing liver cancer research suggests that a number of microbiota signatures are enriched in the tumor regions of the liver in comparison to non-tumor regions of the liver, indicating bacterial translocation.[77] The tumor-associated microbiota included members of the Bacteroidetes, Firmicutes, and Proteobacteria phyla. Interestingly, propionate levels have been linked to reduced liver cancer cell proliferation.[78] A study in a murine proB Ba/F3 model demonstrated that prebiotic treatment was associated with reduced cancer cell proliferation *in vivo* which correlated with increased propionate in the portal vein and lowered systemic inflammation.[79] Further, propionate inhibited the proliferation of the proB Ba/F3 cancer cell line *in vitro*. Collectively, these data suggest that the microbiome and its metabolites can influence the development and severity of liver disease.[52]

Aging and the microbiome

Microbiome transplants from aged donor flies to young recipient flies have been demonstrated to reduce longevity. Similarly, transplants from young fish to aged fish have been shown to increase lifespan.[80] Core-bacteria in humans across different life stages (adults, elderly, centenarians, supercentenarians) demonstrated remarkable

overlap yet could be separated by PCoA analysis.[81] The core-bacteria across all four age groups were the families *Bacteroidaceae, Lachnospiraceae,* and *Ruminococcaceae*. In relatively healthy older adults a decrease in the families *Lachnospiraceae* and *Ruminococcaceae*, and the genera *Coprococcus*, *Roseburia*, and *Faecalibacterium* was observed. *Faecalibacterium* is suggested to have anti-inflammatory properties[66,67] and both *Roseburia* and *Coprococcus* are SCFA producers, which also have anti-inflammatory properties. In another study with older Chinese adults and centenarians[82], centenarians had increased levels of *Roseburia* genus and decreased levels of *Faecalibacterium, Lactobacillus, Coprococcus,* among others. Importantly they found that the abundances of specific microbiota were also dependent on dietary intake of older adults, particularly fiber. They demonstrated that multiple members (8) of the Bacteroides phylum were significantly decreased with high-fiber diet, while (6) members of the *Ruminococcaceae* family, which belong to the *Clostridium* XIVa cluster and are potent SCFA producers, were positively associated with fiber intake. Finally, redundancy analysis of microbiomes from centenarians, elderly, and young adults resulted in discrete clusters.[83] An enrichment of facultative anaerobes, primarily Proteobacteria, and a loss of *Roseburia* and *Faecalibacterium prausnitzii* was observed in centenarians in comparison to non-centenarians, interestingly, a positive association between the gain in Proteobacteria and loss of *Roseburia* and *Faecalibacterium prausnitzii* and IL-6 and IL-8 levels was observed.

Cross-sectional aging studies have also demonstrated that both diet and health status (i.e. frailty, comorbidities) correlate with gut microbiota composition.[9] Older individuals who were community dwelling had a higher proportion of Firmicutes and lower proportion of Bacteroidetes in comparison to subjects in long-term residential care. At the genus level, *Coprococcus* and *Roseburia* were higher in community dwelling older adults, while *Anaerotruncus* and S*treptococcus* were higher in long-stay subjects. Interestingly they found that dietary habits could, in part, explain differences in microbiome composition.[9] Finally, large interindividual variability has been observed in the microbiomes of older individuals,[84] indicating increasing personalization with age. Further, a decrease in the Firmicutes/Bacteroidetes ratio has been observed with increasing age,[85] and is suggested to be an important index of the health of gut microbiota.[86] However, these studies are all cross-sectional in nature, and cannot assess whether these associations are causal. Given the difficulty of conducting human

aging studies, an aging mouse model may be a more appropriate model to address this question despite its inherent limitations.[87]

Sphingolipids, obesity, liver disease, aging and the microbiome

In recent years the study of sphingolipids and their role in aging[88,89] as well as in metabolic diseases[90] have intensified. Sphingolipids have important functions in cellular membranes and as signaling molecules.[91,92] Sphingolipids include signaling molecules such as ceramide (Cer), Cer-1-phosphate, sphingosine, or sphingosine-1-phosphate (S1P) and structural molecules such as sphingomyelin (SM), which in addition to being part of the lipid membrane can also be hydrolyzed to form Cer. Cer can also be made through the *de novo* pathway in the endoplasmic reticulum from serine and palmitoyl CoA. De novo synthesis is regulated by serine palmitoyltransferase (*Spt*).[90] Cer is then transported to the Golgi where it can be deacetylated by ceramidases (Asah) to make sphingosine,[90] which can subsequently be phosphorylated to make S1P, a pro-survival signaling molecule.[93] Cer can also be utilized to synthesize SM in the Golgi via SM synthase (SMS).On the other hand, SM can be hydrolyzed to produce Cer via sphingomyelinase (SMase), SMase's are broken up into three main categories: acid(a), alkaline(ak) and neutral (n)SMase's.[92,94] aSMase works in the lysosome, nSMase's work primarily in the plasma membrane, and akSMase is expressed only in the intestine and liver to help digest dietary sphingolipids.

In aging, elevated levels of ceramide have been found in senescent cells[88] Further, it has been demonstrated that acid ceramidase (*Asah1*) is highly upregulated in senescent cells and silencing of *Asah1* decreased the levels of senescence proteins (p16, p21, p53) and sensitized them to senolytics.[95] Levels of S1P, which promotes cellular proliferation and survival, have also been linked to cellular senescence and cancer. Interestingly, reduction in S1P levels or downregulation of the kinase that phosphorylates sphingosine, *Sphk1/2*, has been shown to promote cellular senescence. However, high levels of Cer C16:0, SM C16:0, sphingosine, and sphinganine were also observed in senescent cells.[96] Increased nSMase activity, and to a lesser extent aSMase, has been linked to senescence as well.[97] Further, the provision of endogenous ceramide to young cells recapitulated a similar proliferative profile as senescent cells.

Sphingolipids can promote proliferation or apoptosis and therefore a delicate balance between pro-survival (i.e. S1P) and -apoptotic (i.e. ceramide, sphingosine) sphingolipid species must be struck.[98] Ceramide generation is involved in stress-induced apoptosis,[99] and generation of ceramide can be triggered by pro-inflammatory and pro-apoptotic stimuli such as TNF-α, ultraviolet light, etc.[93] While inhibition of cellular senescence can help maintain proliferative capacity in old age, old age is also associated with an increased risk for developing cancer. Cancer cells are highly proliferative and thus favor pro-survival and -proliferative signals. S1P has been demonstrated to exert pro-survival effects on cancer cells, promoting proliferation, migration, and inhibiting ceramide-induced apoptosis.[100] Increased levels of Asah1 have also been linked to cancer cells,[101,102] and inhibition of Asah1 promoted the activity of antitumoral agents.[101] Given that the conversion of ceramide and sphingosine to S1P simultaneously removes a pro-apoptotic signal and creates a pro-survival signal, the balance of "sphingolipid rheostat" is a critical determinant of cell fate and is often co-opted by cancer cell to support their growth and expansion.

In obesity, plasma sphingolipids are used as a biomarker for insulin resistance and steatosis.[103–105] The short chain Cer species C16:0 and C18:0, which are produced predominantly by the adipose and liver tissue, are correlated tightly with insulin resistance and steatosis.[106] Elevated levels of plasma SM's have also been suggested to be a putative biomarker/risk factor for the development of atherosclerosis[107] and circulating Cer levels have been suggested to predict major adverse cardiac events.[108] In metabolic diseases over expression of *Asah* attenuated cell death and the inflammatory response after myocardial infarction.[109] Elevations in circulating S1P have also been linked to obesity and metabolic abnormalities (i.e. insulin resistance) in both humans and mouse obesity studies.[110] Adipocyte treatment with S1P has been demonstrated to be proinflammatory.[111] However, in the context of metabolic syndrome and cardiovascular diseases, S1P has also been demonstrated to have protective actions on the cardiovascular systemic,[112] anti-inflammatory actions on macrophages,[113] and is implicated in the metabolically protective actions of adiponectin.[114] While S1P may have protective effects in pathological stress settings, such as obesity, by acutely improving cell survival, however, its anti-apoptotic and pro-angiogenic properties may promote the development of cancer under chronic stress conditions.[115] This conclusion is supported by the fact that obesity is associated with an increased risk of certain cancers, such as

liver cancer.[116] Given that the development of cancer is age-related, the body may increase its levels of S1P to prevent cell death in the short-term, but the increase in S1P in the long term may inadvertently lead to an increased risk of cancer.

Recent developments in the microbiome field have demonstrated that bacteria of the Bacteroidetes phylum can affect the host sphingolipidome.[117] Members of the phylum have been demonstrated to encode *Spt,* which allows them to produce sphingolipids. Bacteroidetes phylum accounts for a significant percentage (20-40%) of the gut microbiome in mice and humans.[118] Members of the *Bacteroides* genus can produce odd-chain sphinganine as well as even-chain length sphinganine, which are similar or identical to mammalian-made even-chain sphinganine.[119] Furthermore, bacteria-derived sphingolipids have been recently demonstrated to alter inflammation homeostasis in the colon,[120] regulate colonic invariant natural killer T cell function,[121] and a strain of *Bacteroides* has been demonstrated to affect host hepatic sphingolipid metabolism.[117] This strain is also able to produce SM *de novo*, which is usually present only in higher animals.[119] Interestingly, *Bacteroides* dominated enterotypes have previously been linked to higher levels of gut inflammation in mice[122] and were positively associated with levels of Proteobacteria or *Enterobacteriaceae*[122] and *Bacteroides* was positively associated with percentage of meat intake.[123] *Enterobacteriaceae* are known to induce inflammation.[124] The role of the gut microbiome in regulating host sphingolipid profiles is an area of active investigation.

Summary

In summary, the existing literature suggests the following: obesity, liver disease, and aging are associated with different alterations in microbiome composition, with can be modified by diet composition. Obesity and development of fatty liver is associated with increased Firmicutes/Bacteroidetes ratio. Increased Firmicutes abundance leads to an increase in energy harvest from our food due to their increased capacity to produce SCFAs which can promote weight gain. Additionally, increased Firmicutes abundance is associated with alterations in the expression of genes involved in fatty acid deposition in the liver. However, SCFAs have anti-inflammatory properties as well as gut barrier integrity promoting properties which may counteract the effects of a high-fat diet. Aging is associated with a reduction in the Firmicutes/Bacteroidetes ratio, however, diet and living situation modify this age associated effect, with older adults living in senior homes,

which were shown to have reduced health status, having lower levels of Firmicutes. Further, both obesity and liver diseases, such as liver cancer and fatty liver, are associated with increased members of harmful and inflammation-inducing bacteria such as *Enterobacteriaceae* and *Streptococcus*. Aging is also associated with increased members of harmful bacteria such as *Enterobacteriaceae* and *Streptococcus* as well. Obesity, aging, and liver cancer are also associated with alterations in sphingolipid metabolism, although the directionality of the changes in the specific species appears to be context specific. In obesity, increases in circulating levels of sphingomyelin and ceramide, and liver ceramide are observed. In aging, increases in ceramide have been observed. Additionally, emerging evidence suggests that the microbiome, i.e. the *Bacteroides* genus, may be a regulator of host sphingolipid metabolism, and if paired with high-fat diet feeding, may lead to increased hepatic levels of ceramide. Given that diet can regulate the composition of the gut microbiome, and favorable associations have been made with F&V intake we hypothesize that lifelong F&V intake could be leveraged to alter the composition of the microbiome by promoting the colonization of SCFA producers, attenuate colonization of putatively harmful bacteria, prevent loss of F/B ratio, attenuate systemic inflammation, and favorably affect the host sphingolipid profile, which, together, should promote healthy aging. Further, given the impact of obesity on host health status, we expect that the effect of F&V will be most dramatic/impactful on obese mice.

Methods

Study design

We tested our hypothesis by using samples that were collected from our recently completed longitudinal study in which 4-week old C57BL/6 mice were randomized into four groups, low-fat (LF-C, 10% kcal fat, n = 60) or a high-fat diet (HF-C, 45% kcal fat, n = 60), and each base diet was supplemented with a F&V mixture equivalent to 6-8 servings of F&V, referred to as LF-FV (n = 60) and HF-FV (n = 60). Mice were fed the respective diet until one group reached 50% median mortality, after which all mice were sacrificed.

Animals

Four batches of C57/BL6 male mice were purchased from Jackson labs and housed at the animal care facility at USDA Human Nutrition Center on Aging at Tufts University.

Each batch was purchased 2-3 weeks apart. Mice were allowed to acclimate for 1 week and placed on a LF diet for 1 week prior to randomization to the 4 groups (LF-C, LF-FV, HF-C, and HF-FV). Mice were maintained in HEPA-filtered ventilated cages located in AAALAC-accredited facilities with an environmentally controlled atmosphere [22°C, 45% relative humidity, and a 12/12-h light/dark cycle (from 07:00 on)] and had free access to diet and water. The protocols for all animal experiments were approved by the IACUC of Tufts University.

Food

LF (10% kcal from fat, #D12450H) and HF (45% kcal from fat, #D12451M) diets were purchased from Research Diets. Each diet was supplemented with 15% F&V powder mix (w/w), corresponding to LF diet with F&V (LF-FV) and HF diet with F&V (HF-FV). F&V mixture was made from the 24 F&V most consumed in the U.S. The mixture was provided by Futureceuticals (Momence, IL). The calorie-normalized levels of micronutrients, protein, and fiber in the LF diet were the same as those in the HF diet and the difference in fat was balanced by varying the amount of carbohydrates. The energy density, protein, and fat levels were similar between F&V supplemented diets and their non-supplemented control.

Table 1. Composition of base diets

	High-fat diet (HF)		Low-fat diet (LF)	
	Product #D12451M		Product #D12450HM	
Macronutrient	per gram %	kcal%	per gram %	kcal%
Protein	24	20	19.2	20
Carbohydrate	41	35	67.3	70
Fat	24	45	4.3	10
Total		100		100
kcal/gm	4.73		2.85	

Diet / Group	F&V content (% w/w)	Protein (kcal %)	Carb (kcal %)	Fat (kcal %)	Energy density (kcal/g)

LF-C	0	20	70	10	3.82
LF-FV	15	18.7	72.17	9.08	3.73
HF-C	0	20	35	45	4.70
HF-FV	15	18.7	41.03	40.33	4.56

Fecal collection

Fecal samples were collected at baseline, 6, 16, and 21 months. The fecal samples collected at baseline were collected 1 week after acclimation and post-randomization, but prior to diet-feeding. For baseline, 6- and 16-months fecal collections, fecal pellets were collected. However, for 21 months, fecal pellets and feces in the colon were collected and combined. Fecal samples were stored at -80°C. At the conclusion of the study, fecal samples were shipped to the University of New Hampshire, Hubbard Center for Genome Studies for 16S rRNA sequencing. The collection time points reflect an estimated human age group of ~10 yrs, 30, 50, and 65 yrs of age. Our fecal sampling, particularly at the 6-month timepoint, was severely hindered by COVID-19 restrictions which reduced our sample size for sequencing and SCFA analysis.

Animal Sacrifice and blood, liver, colon tissue collection

Upon the first group reaching median lifespan (50% mortality), all mice were sacrificed via cervical dislocation post cardiac puncture. Whole blood was allowed to coagulate at room temperature and centrifuged at 2000 x g for 10 min at 4°C. The resulting supernatant (serum) was collected, stored at -80°C, and used for cytokine, lipids, and sphingolipid analyses. Subsequently, the liver was collected, flash frozen with liquid nitrogen, and stored at -80°C for later use. The colon was opened, washed twice with PBS, and subsequently flash frozen with liquid nitrogen, and stored at -80°C for later use. Additionally, blood was collected at 12 months via a retro-orbital bleed to be used for plasma cytokine and sphingolipid analyses.

DNA extraction and sequencing

Bacterial genomic DNA was extracted from each fecal sample using the MagMAX™ Microbiome Ultra Nucleic Acid Isolation Kit (ThermoFisher Scientific). PCR primers targeting the 16S rRNA gene (V4 region) were used to prepare amplicon libraries.[125] Amplification of the 16S V3-V4 region was performed using sequence specific regions in

a dual indexed PCR approach. 16S rRNA sequencing was performed on the Illumina NovaSeq 6000 platform at the UNH sequencing core.

Quality control, merged paired end reads, and taxonomy assignment

Quality control, merging of paired end reads, and taxonomy assignment was performed using the DADA2 pipeline on the Tufts High Performance Computing Cluster. The SILVA database (silva_nr99_v138.1_train_set.fa.gz) was used for general taxonomic assignment of the 16S rRNA data at Kingdom, Phylum, Class, Order, Family and Genus levels. Libraries with a low sequencing depth (< 4000 reads) or sequences which were host-derived (e.g. mitochondrial sequences) were removed.

Liver homogenization

Frozen liver tissue was pulverized. Pulverized liver tissue was subsequently aliquoted into 3 screw-cap homogenization tubes for cytokine, gene expression, and sphingolipid analysis.

Colon homogenization

Frozen proximal colon tissue was pulverized and aliquoted into 2 screw-cap homogenization tubes for cytokine and gene expression analysis.

Serum and liver ceramides

Blood and liver tissue lipidomic profiles were analyzed using LC-tandem MS (AB SCIEX 4000 QTRAP) as previously reported by Virginia Commonwealth University Massey Cancer Center Lipidomics Shared Resource.

Serum cytokines/inflammation

To determine systemic inflammatory milieu, we used serum isolated from whole blood. Whole blood was centrifuged at 2000 x g for 10 min at 4°C and the resulting supernatant was collected, stored at -80°C, and used for cytokine analysis using an ELISA-based multiplex kit (Mesoscale).

Liver and colon mRNA extraction

Liver and colon mRNA were extracted using the Trizol-based method. Briefly, ~50-100 mg of tissue was homogenized in Trizol. RNA was extracted from the Trizol mix using

chloroform. The upper clear aqueous phase was collected, and the RNA was precipitated using isopropanol. Pelleted RNA was washed twice with 75% ethanol, air-dried, and resuspended in RNAsecure.

Liver and colon nano-drop and cDNA synthesis

The purity and amount of purified RNA was determined using a NanoDrop Spectrophotometer (ThermoFisher). 2 µg of RNA was used to synthesize cDNA using the SuperScript IV First-Strand Synthesis Kit (ThermoFisher) according to the manufacturer's recommendations.

Liver and colon gene expression, qPCR

qPCR was performed on an ABI QuantStudio 12K Flex (ThermoFisher, Waltham, MA) using SYBR Green (ThermoFisher, Waltham, MA). ΔΔCT was used to estimate relative changes in mRNA transcript abundance of genes of interest with *Hprt* as the housekeeping control.

Table 3. Primer sequences

Gene	Sequence
Smpd1	F: 5'-GTTACCAGCTGATGCCCTTC-3'
	R: 5'-AGCAGGATCTGTGGAGTTG-3'
Smpd2	F: 5'-AGCAGGATCTGTGGAGTTG-3'
	R: 5'-CTCCAGCCATGAAGCTCAAC-3'
Smpd3	F: 5′-GCAGGAGGTGTTTGACAAG-3′
	R: 5'-TCTTTGGTCCTGAGGTGTG-3'
Smpd4	F: 5'-ACCTGGCCCTCAATCCATTTG-3'
	R: 5'-ATAGGCACAGTCCGAAGTACG-3'
Sgms2	F: 5'-CTGGGATCATCTGCATTCTC-3'
	R: 5'-GTTCGTCTGGGAAGAGACCT-3'
Sphk1	F: 5'-ACAGCAGTGTGCAGTTGATGA-3'
	R: 5'-GGCAGTCATGTCCGGTGATG-3'
Sphk2	F: 5'-AGACGGGCTGCTTTACGAG-3'
	R: 5'-CCTGCTCAAACCCGCCAT-3'
Cers2	F: 5'-CATGGCTGTCACTGTGGATAA-3'
	R: 5'-GAAGGGATGATGCTCTGTATGG-3'
Sptcl1	F: 5'-AGGGTTCTATGGCACATTTGATG-3'
	R: 5'-TGGCTTCTTCGGTCTTCATAAAC-3'
Sptcl2	F: 5'-CAAAGAGCTTCGGTGCTTCAG-3'
	R: 5'-GAATGTGTGCGCAGGTAGTCTATC-3'
Asah1	F: 5'-TTGACCTTTGGTAACATCCATC-3'
	R: 5'-TAACCGCAGAACACCGGCC-3'
IL-10	F: 5'-GCTCTTACTGACTGGCATGAG-3'
	R: 5'-CGCAGCTCTAGGAGCATGTG-3'

IL-10Ra	F: 5'-GTTTCTGGGCAGAGAGGGTT-3'
	R: 5'-CCTGGTCTGTCTGGTTCTCC-3'
Muc2	F: 5'-ATGCCCACCTCCTCAAAGAC-3'
	R: 5'-GTAGTTTCCGTTGGAACAGTGAA-3'
ZO-1	F: 5'-GCAGACTTCTGGAGGTTTCG-3'
	R: 5'-CTTGCCAACTTTTCTCTGGC-3'
Occludin	F: 5'-AGACTACACGACAGGTGGGG-3'
	R: 5'-CTGCAGACCTGCATCAAAAT-3'
Claudin 7	F: 5'-TGATGAGCTGCAAAATGTACG-3'
	R: 5'-GCCTTCTTCGCTTTGTCATC-3'
Claudin 2	F: 5'-TTCGCCTTTCTCTGGACCTA-3'
	R: 5'-TCACAGTGTCTCTGGCAAGC-3'
IL-6	F: 5'-CCAGTTGCCTTCTGGGACT-3'
	R: 5'-GGTCTATTGGGAGTGGTATCC-3'
TNFα	F: 5'-ATGGGCTTTCCGAATTCAC-3'
	R: 5'-GAGGCAACCTGACCACTCTC-3'
Lbp	F: 5'-ACTTCAAGATCAAGGCCGTGG-3'
	R: 5'-CACCGATGGAAGAGTCAGAGA-3'

Liver and colon cytokines/inflammation

To determine liver and colonic inflammation, we homogenized liver and colon tissue using an Omni Bead Ruptor 12 (OMNI International, Kennesaw, Georgia) in a Tris-based buffer with protease and phosphatase inhibitors. The resulting homogenate was centrifuged for 10 min at 10,000 x g and 4°C. The supernatant was collected, and stored at -80°C. We determined cytokine levels using ELISA kits (R&D) according to the manufacturer's recommendations. The resulting signal was read on a BioTek EL808 plate reader (BioTek Instruments, Winooski, VT)

Fecal short chain fatty acids

Fecal short chain fatty acid concentrations were measured using LC-MS by the Arkansas Children's Hospital Metabolomics Core. Approximately 100 mg of fecal samples was dried and homogenized in 50% aqueous acetonitrile spiked with internal standards. Chromatographic separation was performed on an ACQUITY Premier UPLC and quantification were carried out on a SELECT SERIES Cyclic IMS (Waters, Milford, MA) using the full scan QToF data acquisition mode. Fecal short chain fatty acid concentrations were normalized to the wet weight of the fecal pellets. Fecal short chain fatty acid concentrations were determined using pooled fecal samples from 2-4 mice/group.

Data Analysis

16S rRNA quality control - Prior to analysis, the 16S rRNA data was denoised, paired ends were merged, and chimeras and host-derived sequences removed. We were left with an average of 54,594.87 reads. We removed samples which had a read count less than or equal to 4,000 reads, bringing the average number of reads to 61,918.57. These curated reads were used for all further analyses. See below, a breakdown of the read counts by group and time point.

Table 4. Amplicon read counts by group and time point

Group	Time point (months)	Mean number of reads	n	SE
LF-C	0	25,354.4	55	2,130.1
	6	56,693.6	43	4,125.6
	16	67,766.9	48	5,829.6
	21	23,242.4	39	3,322.1
LF-FV	0	86,812.8	48	14,421.7
	6	61,630.9	43	3,202.3
	16	49,334.9	45	5,134.8
	21	38,377.4	44	3,085.8
HF-C	0	204,214.1	58	21,259.4
	6	51,920.4	44	3,202.6
	16	47,803.3	37	4,793.4
	21	40,237.9	28	5,585.7
HF-FV	0	68,797.5	57	5,742.7
	6	47,217.5	34	5,322.2
	16	10,540.6	23	1,734.3
	21	20,169.5	35	2,483.4

β-diversity

To determine dissimilarity in microbial community composition across diet groups and timepoints, we calculated β-diversity values using the vegan R package. To determine differences in the centroids we used Permutational multivariate analysis of variance (PERMANOVA). Dissimilarity values were then extracted from the dissimilarity matrix and used to determine patterns in inter-individual variability with time and between groups. To determine statistical significance in the variability of β-diversity with time and across groups we used a general linear model.

MassLin2

To determine longitudinal differences in age- and diet-associated microbiota, we used the MassLin2 R package. To account for repeated measures inherent in our longitudinal study design we set “Mouse ID” as a random effect. To identify diet-associated differentially abundant taxa between the LF-C vs LF-FV and LF-C vs HF-C groups we used the LF-C group as our reference group for both comparisons. To identify diet-associated differentially abundant taxa between the HF-C vs HF-FV, we used the HF-C group as our reference group. For determining age-associated differentially abundant taxa, we coded our time points/age as a continuous variable (0, 6, 16, 21 months). The resulting p-values were adjusted for multiple comparisons using the Benjamini-Hochberg method. An adjusted p-value (q-value) <0.05 was considered statistically significant. Our data was provided as a count matrix, which was subsequently normalized using the total sum scaling method (TSS) and the resulting TSS values were log transformed. Age- and diet-associated microbiota were subsequently used for omic data integration.

Firmicutes/Bacteroidetes ratio

To determine the Firmicutes/Bacteroidetes (F/B) ratio we used both the TSS-normalized count values and relative percentage. Group differences were assessed using the Kruskal-Wallis rank sum test. If the resulting p-value was significant, we performed pairwise comparisons using the Wilcoxon rank sum test and corrected for multiple comparisons using the Benjamini-Hochberg method. To determine if the F/B ratio changed with age we used a mixed effects regression model.

Fecal short chain fatty acids

Fecal short chain fatty acid (SCFA) levels were normalized to the weight of the fecal pellets. Values were checked for normality and if values were not normally distributed,

they were transformed. Differences in SCFA levels between groups were determined using a one-way ANOVA followed by a Student's t-test with a Tukey adjustment. The comparisons of interest were LF-C vs HF-C, LF-C vs LF-FV, and HF-C vs HF-FV.

Gene expression & cytokine analysis

Differences in the gene expression or levels of cytokines in colon and liver tissue was assessed across the diet groups using a one-way ANOVA followed by a Student's t-test with a Tukey adjustment. The comparisons of interest were LF-C vs HF-C, LF-C vs LF-FV, and HF-C vs HF-FV.

Sphingolipids

To determine diet differences in sphingolipid species in circulation and the liver, we first normalized and mean-centered the data. Diet differences were then assessed by one-way ANOVA followed by Student's *t*-test with a Tukey adjustment. The comparisons of interest were LF-C vs HF-C, LF-C vs LF-FV, and HF-C vs HF-FV.

Omic data integration

Circulating and liver sphingolipids, fecal microbiome, and systemic inflammation were integrated using the MixOmics R package. These data were all from the 21-month time point. Only the age- and diet-associated taxa identified in the MassLin2 analysis were used for integration. The sphingolipidomic and inflammatory datasets were normalized and mean-centered using the "autoscale" function in the "mdatool" R package. The microbiome dataset was normalized by the TSS method, using the "decostand" function in the vegan R package. The normalized datasets were then parsed into the mixOmics R package.

Liver cancer - associations

To determine the number of components to use we first fit a multiblock PLS-DA model without variable selection and set the number components to 5 and the "nrepeat" to 30. Using the overall balanced error rate, we determined that 2 components were sufficient. We then set the minimum and maximum number of variables for each block. For the microbiome "block" we set a limit of 22 features (out of 56 features (55 taxa and the Firmicutes/Bacteroidetes ratio)), for both sphingolipid "blocks" we set a limit of 18 features (out of 37 species), and for the cytokine "block" we set a limit of 3 features (out

of 5). To increase our confidence in our model, we set the “nrepeat” to 30 in the “tune.block.splsda” function. The tuning step reported the following number of features for each block: the liver sphingolipid, 16 and 14 features, for components 1-2; the circulating sphingolipid “block”, 18 and 5 features, for components 1-2; the microbiota “block”, 10 and 18 features, for components 1-2; the cytokine “block”, 1 and 1 feature, for components 1-2. To plot the associations/interactions across the datasets we focused on strong associations (correlation cutoff = 0.65).

Chapter 1: Lifelong fruit and vegetable intake results in gut-microbiome remodeling

Preface: As mentioned previously, this thesis leveraged samples from a recently completed longitudinal mouse study designed to test the effect of F&V on health span and lifespan. In this 21-month study, mice fed a high-fat (HF) diet without F&V supplementation (HF-C) were the first to reach 50% mortality. Importantly, no difference in mortality between low-fat (LF) diet fed control mice (LF-C) and mice fed a high-fat diet with F&V supplementation (HF-FV) was observed.[11] Furthermore, tumor incidence was significantly higher in the HF-C group (73.3%) in comparison to LF-C (30.0%), primarily driven by an increased incidence in liver cancer. HF-FV had 23.3% lower tumor incidence in comparison to the HF-C group. To determine potential mechanisms, we assessed gut microbiome composition, systemic inflammation, and systemic and liver sphingolipid profiles.

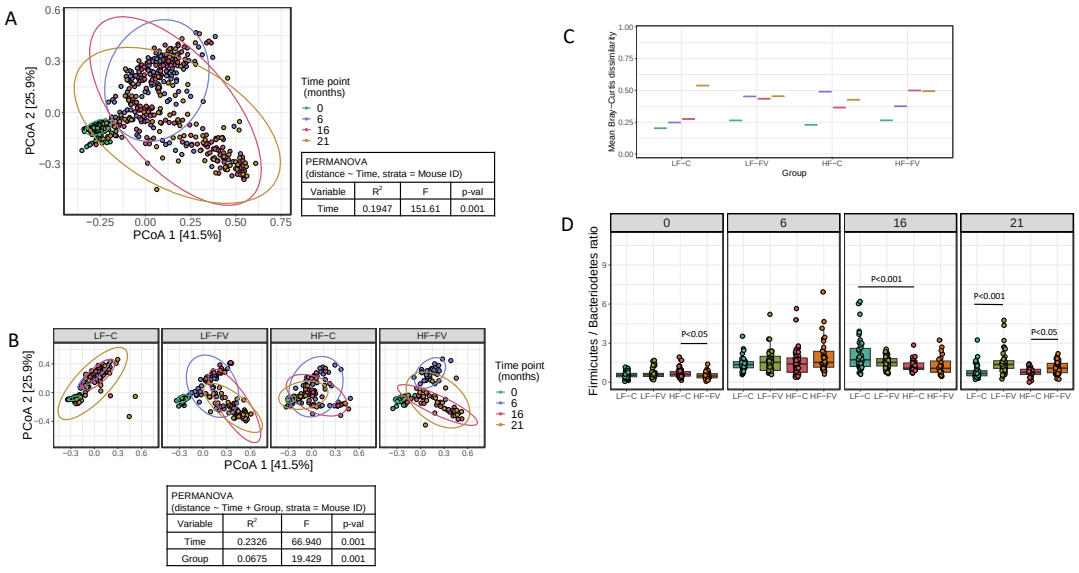

Panel 1: Features of the gut microbiome vary by diet and age. A) Principal component analysis (PCoA) of β-diversity values according to age/life stage, B) PCoA of β-diversity values according to age/life stage and diet, C) Inter-mouse β-diversity variability within each group at different life stages, and D) Firmicutes/Bacteroidetes ratio across life stages and groups. Permutational multivariate analysis of variance (PERMANOVA) was used to determine differences between the centroids. The drawn error ellipses assume a normal distribution. Group differences in inter-mouse β-diversity variability were assessed using one-way ANOVA followed by Student's t-test and post-hoc adjustment for multiple comparisons, as well as a mixed effects regression.
Firmicutes/Bacteroidetes (F/B) ratio was calculated using the normalized (TSS) values, differences in ratios were determined using one-way ANOVA followed by Student's t-test and post-hoc adjustment for multiple comparisons, as well as a mixed effects regression.

To determine if the microbiomes of mice changed with respect to age, we calculated a β-diversity value for each of the fecal samples collected across all groups and life stages. As shown in Figure 1A, we observed tight-clustering of β-diversity values at early age ("0"), suggesting that the microbiome composition of different mice was more similar than dissimilar, despite the β-diversity values originating from 4 different sets/batches of mice. With increasing age, the tight-clustered β-diversity values became increasingly dispersed. To test if the centroids for each timepoint were statistically different from one another we used permutational multivariate analysis of variance (PERMANOVA). The results of the PERMANOVA were significant ($P<0.001$), indicating that the centroids were statistically different from one another. The R^2 value of this PERMANOVA model was 0.194, indicating that time/age explained 19.4% of the variability observed in the spread of β-diversity values.

To determine if the microbiomes of mice changed with respect to diet, we overlaid the "Group" information onto our existing PCoA plot (Supplementary Figure (SFig) 1A). A PERMANOVA was performed with respect to diet group (distance ~ group) and the results revealed an insignificant effect of diet on the spread of β-diversity values ($P = 1$). We suspected that the effect of diet on gut microbiome community composition would depend on life-stage, thus, we adjusted our time-dependent PERMANOVA model with the "Group" variable (distance ~ Time + Group). Indeed, as shown in Figure 1B, diet was statistically significant ($p < 0.001$) when accounting for life-stage and the R^2 value of this

PERMANOVA model was 0.067, indicating that diet/group explained 6.75% of the variability observed in the spread of the β-diversity values. Together, our β-diversity analysis suggests that aging is a strong determinant of microbial community structure while diet is a modest determinant.

Importantly, we tested whether the “batch” number (1-4) was an important determinant of microbial community structure. As shown in Supplementary Figure 1B effect of “batch” in our adjusted PERMANOVA model (distance ~ Batch) was insignificant ($p = 1$) and the accompanying R^2 was 0.017, indicating that diet/group explained approximately 1% of the observed variability in our β-diversity values.

We then calculated the Firmicutes/Bacteroidetes (F/B) ratio, which is typically reduced with age, owing to the loss of the Firmicutes phylum. In our mixed effects regression analysis, we observed that coefficient for age was positive ($P<0.001$), suggesting that in our aging mouse model, F/B increased with age. Diet alone was not significant in affecting the F/B ratio ($P = 0.1$). However, the diet*age interaction term was significant ($P<0.05$), suggesting that the effect of diet depends on age. This observation corroborates our earlier PERMANOVA results which demonstrated that the general composition of the microbiome (assessed by β diversity) was dependent on age alone, but not diet alone. However, addition of the diet term to our age PERMANOVA test was significant, which suggested, again, that the effect of diet on microbiome composition is modest, but likely interacts/depends on age. Interestingly, in our analysis, the coefficient for the HF-C*age was negative (-0.025) indicating that HF-diet alone reduced the F/B ratio with age. The coefficient for the HF-FV*age interaction term was also negative (-0.01) but suggested that lifelong F&V may attenuate the effect of HF-diet on the F/B ratio. Together, these results indicate that changes in F/B ratios depend on age and its interaction with diet.

As shown in Figure 1D, F&V supplemented mice had a significantly higher F/B ratio by the end of the study. This observation was recapitulated using the relative percentage of each phylum (SFig. 2A). Inspection of the relative percentage of each phylum across the groups (SFig2 B-C) demonstrated that the rise or maintenance of the F/B ratio was due to a loss of the Verrucomicrobiota phylum and an increase in Firmicutes in mice supplemented with F&V.

Taken together, our longitudinal microbiome composition analysis (assessed by β-diversity) suggests that diet and age are important determinants of community structure, with mice having more similar community structure than dissimilar ones at an early age. However, with increasing age the microbiomes of some mice became increasingly dissimilar, and diet helps further explain the observed variability. This time-dependent increase in inter-mouse variability can be observed by plotting the dissimilarity values of each mouse within their respective group across the different timepoints, as shown on Figure 1C. Together, these results indicated that diet and age have an important role in determining microbial community composition and that age is associated with microbiome personalization, in agreement with previous cross-sectional diet and aging microbiome studies.

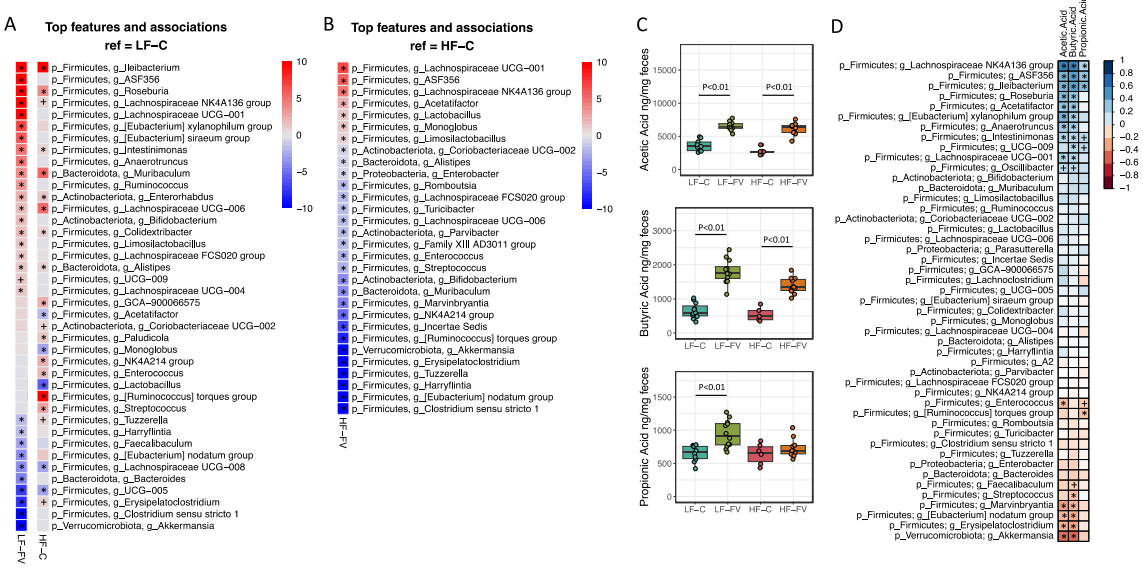

Panel 2: MassLin2 analysis of the microbiome at the genera level reveals loss and enrichment of specific microbiota according to group. A) Diet-associated changes in the microbiome of LF-FV and HF-C relative to LF-C, B) diet-associated changes in the microbiome of HF-FV relative to HF-C, C) fecal short-chain fatty acid concentrations (SCFA) at the end of the study, and D) correlation between fecal SCFA's (ng/mg of feces) and diet-associated microbiota. A-B) The intensity of the color represents the association score (association score = -log(q-value)*effect size). Significant associations (adjusted p-value <0.05) are shown on the heatmap with an asterisk (*), and associations that trend towards significant (adjusted p-value < 0.1) are represented by a

plus sign (+). P-values (q-values) were adjusted for multiple comparisons using the Benjamini-Hochberg method. C) Pooled fecal short-chain fatty acid concentrations were normalized to the wet-weight of the feces and differences in concentrations were determined using one-way ANOVA followed by Student's t-test and post-hoc adjustment for multiple comparisons. D) Spearman's correlation analysis was performed between the TSS values of diet-associated microbiota and the mean-centered and scaled SCFA concentrations, and p-values were adjusted for multiple comparisons using the Benjamini-Hochberg method.

Given that we observed both age- and diet-dependent differences in our PCoA of the β-diversity values, we used the MassLin2 R package to determine which specific taxa were differentially abundant across the diet groups and life-stages.

As shown in Figure 2A, in comparison to LF-C, LF-FV was positively and strongly associated with an enrichment of the *Ileibacterium, ASF356, Roseburia, Lachnospiraceae NK4A136 group, Lachnospiraceae UCG−001, [Eubacterium] xylanophilum group, [Eubacterium] siraeum group,* and *Intestinimonas* genera. Modest enrichment of the *Anaerotruncus, Muribaculum* (previously referred to as *S24-7*), *Ruminococcus, Lachnospiraceae UCG−006,* and *Bifidobacterium,* among other genera. In comparison to LF-C, LF-FV was associated with a reduction in the genera *Akkermansia, Clostridium sensu stricto 1, Erysipelatoclostridium, UCG−005, Bacteroides, Lachnospiraceae UCG-008, [Eubacterium] nodatum group, Faecalibaculum, Harryflintia,* and *Tuzzerella.* Enrichment of the *ASF356, Roseburia, Ileibacterium* and *Lachnospiraceae NK4A136 group g*enera suggested an increased potential to produce SCFA's with F&V supplementation.

In comparison to LF-C, HF-C was positively associated with an enrichment of the *[Ruminococcus] torques group, Ileibacterium, Muribaculum, Lachnospiraceae UCG−006, Roseburia, Enterococcus, Streptococcus*, *Colidextribacter*, *Intestinimonas, NK4A214 group, GCA-900066575,* and *Enterorhabdus* genera. HF-C was negatively associated with *Lactobacillus, Acetatifactor, Monoglobus, UCG-005,* and *Lachnospiraceae UCG−008*. HF-C was the only group associated with a longitudinal enrichment in the *Enterococcus* and *Streptococcus* genera, as well as *[Ruminococcus] torques group*, are implicated to be harmful, inflammation inducing, and associated with liver cancer.[77,126,127]

To confirm the observed F&V-associated enrichment in SCFA producing bacteria we performed SCFA analysis on our remaining fecal samples. As shown in Figure 2C, both F&V treated groups had significantly increased levels of acetic and butyric acid ($P<0.01$) at the end of the study in comparison to their non-supplemented counterparts. Only the LF-FV group had elevated levels of propionic acid ($P < 0.01$) in comparison to the LF-C group. Correlation analysis was performed between SCFA's and diet-associated microbiota. As shown in Figure 2D, the genera *ASF356* and *Lachnospiraceae NK4A136 group,* both which were strongly associated F&V supplementation, were positively and significantly correlated with levels *of* acetic, butyric, and propionic acid. *Roseburia, Ileibacterium,* and *Acetatifactor,* which were enriched in the microbiomes of F&V supplemented mice, were also correlated with levels of acetic and butyric acid. Importantly, *Akkermansia*, *Erysipelatoclostridium,* and *[Eubacterium] nodatum group,* and other microbiota associated with the HF-C group were negatively associated with fecal SCFA's.

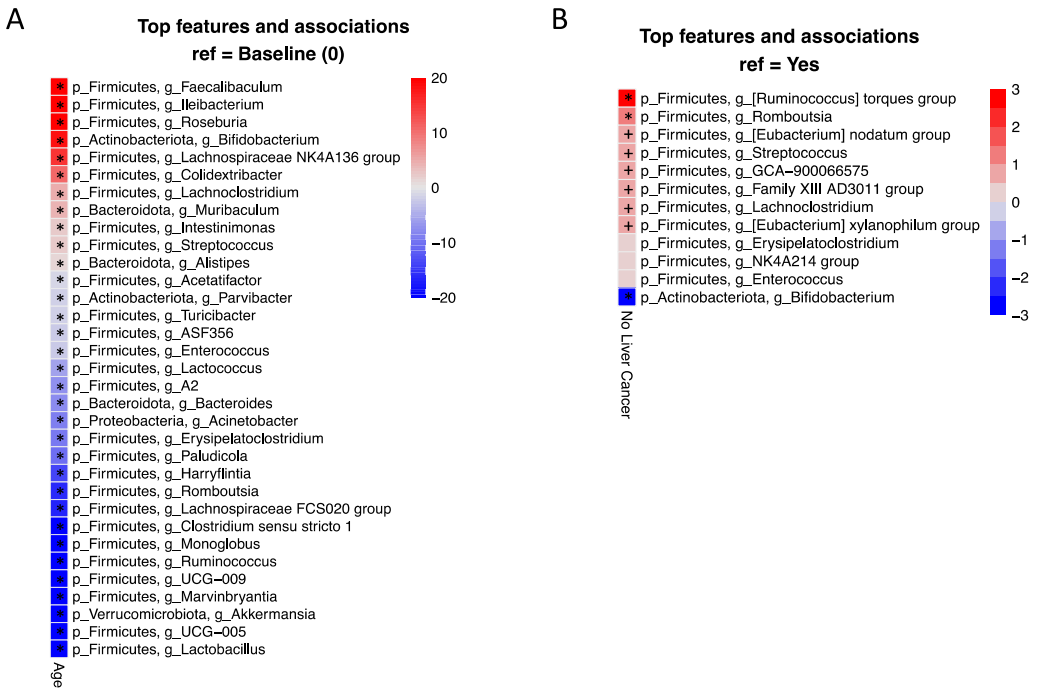

Panel 3: MassLin2 analysis of the microbiome at the genera level reveals loss and enrichment of specific microbiota with age and liver cancer. A) Age-associated changes in the microbiome relative to baseline, and B) microbiota associated with liver cancer

incidence. A-B) The intensity of the color represents the association score (association score = -log(q-value)*effect size). Only significant associations (adjusted p-value <0.05) are shown on the heatmap and are represented by an asterisk (*) and associations that trend towards significance (adjusted p-value < 0.1) are represented by a plus sign (+). P-values (q-values) were adjusted for multiple comparisons using the Benjamini-Hochberg method.

As shown in Figure 3A, a strong age-dependent increase in the levels of *Fecaelibaculum, Ileibacterium, Roseburia, Bifidobacterium,* and *Lachnospiraceae NK4A136 group* genera was observed. While not equal in magnitude, the *Streptococcus* and *Muribaculum* genera were also enriched with age, the former a putatively pathogenic bacteria and the latter a member of the Bacteroidetes phylum. Age-associated increases in *Fecaelibaculum, Roseburia,* and *Lachnospiraceae NK4A136 group* are typically viewed as health-promoting given their anti-inflammatory properties and production of SCFA's[128–130] which may support gut health in the aging mouse, and which may also counteract loss of gut barrier integrity which typically deteriorate with age. Interestingly, age was positively associated with the enrichment of two members of the Bacteroidetes phylum, *Muribaculum and Alistipes*, which were both higher in the HF-C group. The *Bacteroides* genus was negatively associated with age, but this effect is likely driven by the strong negative association with LF-FV. Conversely, *Lactobacillus*, *UCG-005, Akkermansia, Marvinbryantia, UCG-009, Ruminococcus, Monoglobus*, *Clostridium sensu stricto 1, Lachnospiraceae FCS020 group, Romboutsia,* and *Harryflintia* genera were significantly reduced with age in all groups regardless of diet.

Using MassLin2, we next determined which diet- and age-associated microbiota were longitudinally associated with the development of liver cancer. As shown in Fig 3B, *Romboutsia* and *[Rominococcus] torques group* were both positively and significantly associated with the incidence of liver cancer, albeit the effect size (coefficient) was modest. The genera *[Eubacterium] nodatum group*, *Streptococcus*, GCA-900066575, and *Family XIII AD3011 group*, *Lachnoclostridium*, and *[Eubacterium] xylanophilum group* were also positively associated with liver cancer; however, after adjusting for multiple hypothesis testing the adjusted P-value was non-significant but trended towards significance (P < 0.1). Conversely, *Bifidobacterium* was negatively associated with the incidence of liver cancer. Importantly, *Romboutsia* was negatively associated with both

F&V supplemented groups, which may protect mice against liver cancer despite HF-diet feeding. Further, the *Bifidobacterium* genus was positively associated with LF-FV, but negatively associated with HF-FV likely because of HF-diet feeding.

In summary, our analysis of the microbiome suggested that F&V supplementation promoted the longitudinal enrichment of well-known SCFA producers, which was supported by both our quantitation of fecal SCFA concentrations at the end of the study and their strong correlation to F&V associated microbiota. In comparison to HF-diet alone, supplementation with F&V attenuated increases in *Streptococcus, Enterococcus, Erysipelatoclostridium, [Eubacterium] nodatum group, Romboutsia, Family XIII AD3011,* and *Tuzzerella*. These bacteria were predominant present in the HF-C group and were importantly associated with liver cancer incidence. Additionally, we observed that F&V was associated with maintenance of the F/B ratio due to higher levels of Firmicutes in both groups, while in the LF-FV was negatively associated with the *Bacteroides* genus and HF-FV was associated with a reduction in both *Muribaculum* and *Alistipes* of the Bacteroideta phylum.

Given the emerging role of the microbiome, particularly members of the Bacteroideta phylum, in contributing to the regulation of the host sphingolipidome, and the role the sphingolipids play in aging and cancer, we subsequently assessed if F&V was associated with differences in the circulating sphingolipid pool.

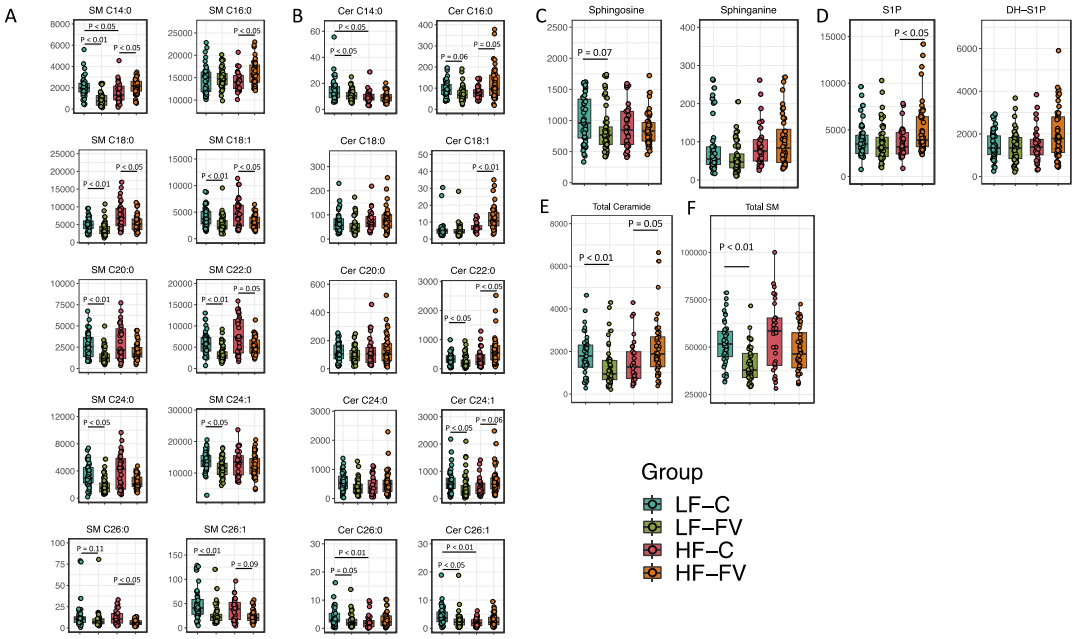

Panel 4: Levels of circulating sphingomyelins, ceramides, and derivatives (pmoles/mL). Differences in concentrations of sphingolipids were determined using one-way ANOVA followed by Student's t-test and post-hoc adjustment for multiple comparisons SM = sphingomyelin, Cer = ceramide, S1P = sphingosine-1-phosphate, DH-S1P = dihydro-S1P.

We determined which sphingolipid species were significantly different between the groups. As shown in Figure 4A, we found significantly lower levels of various circulating sphingomyelins (SM) C14:0, C18:0, C18:1, C20:0, C22:0, C24:0, C24:1, and C26:1 – almost all SM's (except C16:0 and C26:0), were lower in the LF-FV group in comparison to LF-C. Similarly, SM C18:0, C18:1, C22:0, and C26:0 were lower in the HF-FV group, compared to HF-C. A lower level of SM C20:0, C24:0, and C26:1 were also observed, but the difference was not statistically significant. A significantly higher level of SM C14:0 and SM C16:0 levels were observed in the HF-FV, compared to HF-C group. Between HF-C and LF-C, a significant difference in SM C14:0 was observed. These results suggested that F&V supplementation is associated with a reduction in levels of circulating SM's, albeit to a much lesser degree in the HF-FV group. A significant difference in total SM was found between LF-C and LF-FV, although total SM was lower on average in the HF-FV group. Circulating levels of SM's can act as substrates for the

generation of ceramides (Cer) in different tissues and have been suggested to be markers of metabolic disease, thus we next turned our attention to circulating Cer.

The circulating Cer species, Cer C14:0, C22:0, C24:1, C26:1, and in total Cer were significantly reduced in the LF-FV group, in comparison to LF-C (Figure 3B). In contrast, the HF-FV group had higher levels of Cer C16:0, C18:1, and C22:0 in comparison to HF-C. However, all other Cer species were similar between HF-C and HF-FV. Taken together, our data indicates that F&V supplementation is associated with lower levels of SM's. In the LF fed mice FV supplementation was associated with an overall lower level of circulating SM's and Cer species. As shown in Figure 4D, no significant differences in the levels of sphinganine or sphingosine were observed, however, a significant increase in the levels of circulating sphingosine-1-phosphate (S1P) was observed in the HF-FV group in comparison to HF-C.

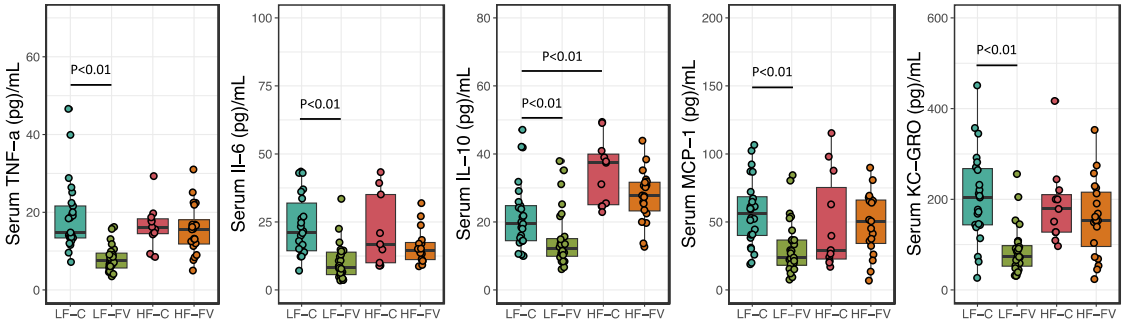

Panel 5: Effect of high-fat diet and F&V supplementation on inflammatory milieu. Differences in the levels of different cytokines (pg/mL) were determined using one-way ANOVA followed by Student's t-test and post-hoc adjustment for multiple comparisons. TNF = tumor necrosis factor, IL = interleukin, MCP = monocyte chemoattractant protein, KC-GRO = Keratinocyte chemoattractant-human growth-regulated oncogene.

Given the robust F&V-associated change in circulating SM and gut microbiota, we next sought to determine the levels of circulating inflammatory markers in response to F&V supplementation. As shown in Figure 5, circulating levels of inflammatory markers, TNF-α, IL-6, IL10, MCP-1, and KC-GRO, were significantly (P<0.01) lower in the LF-FV group in comparison to LF-C. No significant differences in the levels of any cytokines between HF-C and HF-FV were observed, albeit the levels of IL-6 and IL-10 were on average lower in the HF-FV group. HF-C was associated with a significantly higher level of

circulating IL-10, in comparison to LF-C (P<0.01) and no other differences were observed. As an additional comparison, we compared IL-10 levels between HF-FV and LF-C and report no significant difference between the two groups. We conclude that F&V in the background of a LF diet has anti-inflammatory. While on average the level of inflammatory cytokines was lower in the HF-FV compared to HF-C, the difference did not reach statistical significance.

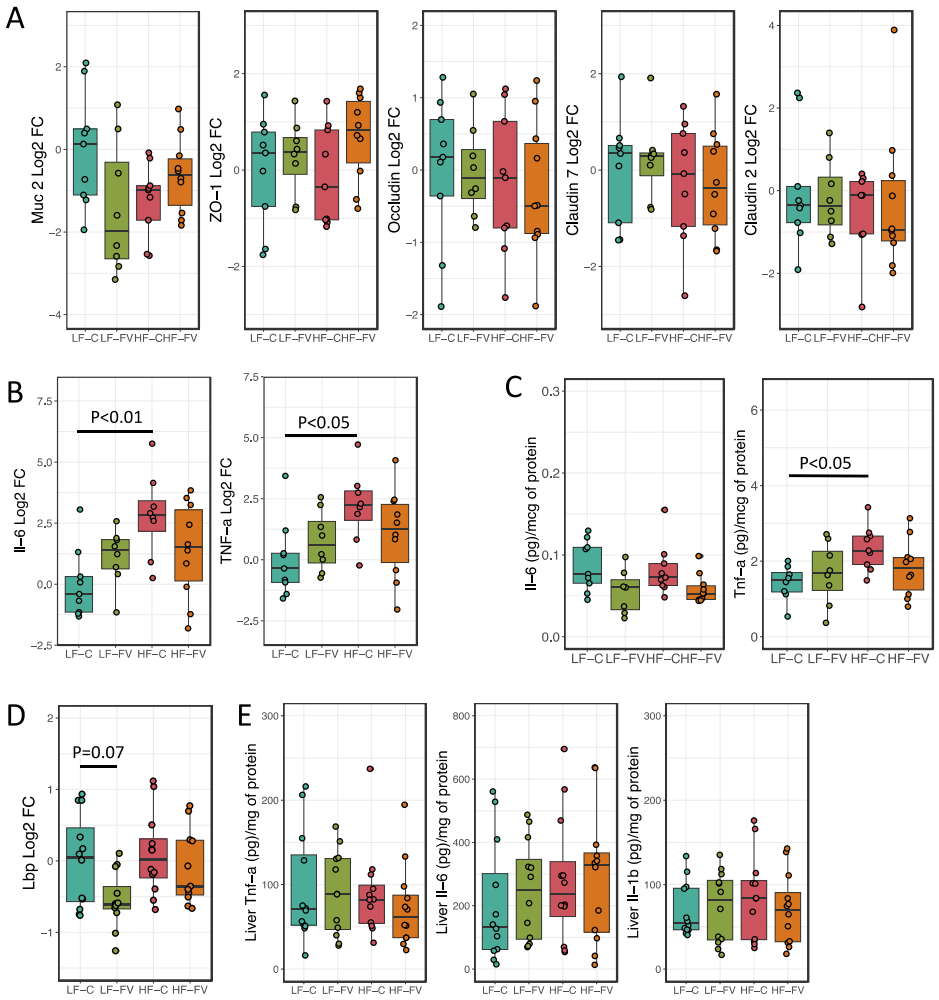

Panel 6: Interrogation of the leaky-gut axis. A) Expression of genes linked to gut barrier integrity, B) colonic inflammation, C) levels of cytokines in the colon (pg/mg of protein), D) expression of liver LPS-binding protein, and E) levels of liver inflammation (pg/mg of protein). Differences in gene expression and concentrations of cytokines were determined using one-way ANOVA followed by Student's t-test and post-hoc adjustment for multiple comparisons.

Given that F&V was associated with lower levels of circulating cytokines, attenuated the enrichment of pathogenic bacteria, such as *Streptococcus*, and had higher levels of fecal SCFA's, we next sought to determine the effect of F&V on gut barrier integrity. HF-diet can promote loss of gut barrier integrity by promoting colonic inflammation and loss of tight-junction integrity. Loss of barrier integrity can lead to bacterial translocation to promote pro-inflammatory processes, that if left unresolved can contribute to liver cancer. As previously shown in Figure 2A-D, F&V was associated with a robust increase in SCFA's, most notably acetic and butyric acid. Previous studies have linked SCFAs with differential expression of genes associated with maintenance of the gut barrier and colon inflammation. As shown in Figure 6A, assessment of the gene expression levels of tight-junction proteins in the proximal colon revealed no significant differences. A significant difference in the gene expression of the inflammatory cytokines TNF-α and IL-6 was observed between HF-C and LF-C groups (Figure 6B). Assessment of protein levels revealed a similar pattern in TNF-α levels, but no differences were observed in IL-6 protein levels (Figure 6C).

Impairments in barrier integrity may lead to the leakage of pro-inflammatory microbial-derived molecules into circulation. As a proxy of exposure to bacterial endotoxin we assessed the expression of the LPS-binding protein (*Lbp*) gene in the liver. As shown in Figure 6D, the expression of *Lbp* was similar across groups, although the LF-FV group trended towards expressing it at lower levels ($P = 0.07$). The lower levels of *Lbp* expression may, in part, contribute to the overall reduction in circulating cytokines. Analysis of liver cytokines revealed no significant differences in TNF-α, IL-6, or IL-1β. Taken together, these results suggest that impaired gut barrier integrity was unlikely to explain differences in liver cancer incidence between HF-C and HF-FV mice. However, the presence of specific microbes, such as *Streptococcus* and *Enterococcus*, which were enriched in the microbial communities of HF-C fed mice, may be a sufficient trigger to the development of liver cancer, despite similarities in the expression of genes involved in barrier integrity. Our data suggests that loss of barrier integrity is unlikely to explain differences in liver cancer incidence between HF-C vs HF-FV.

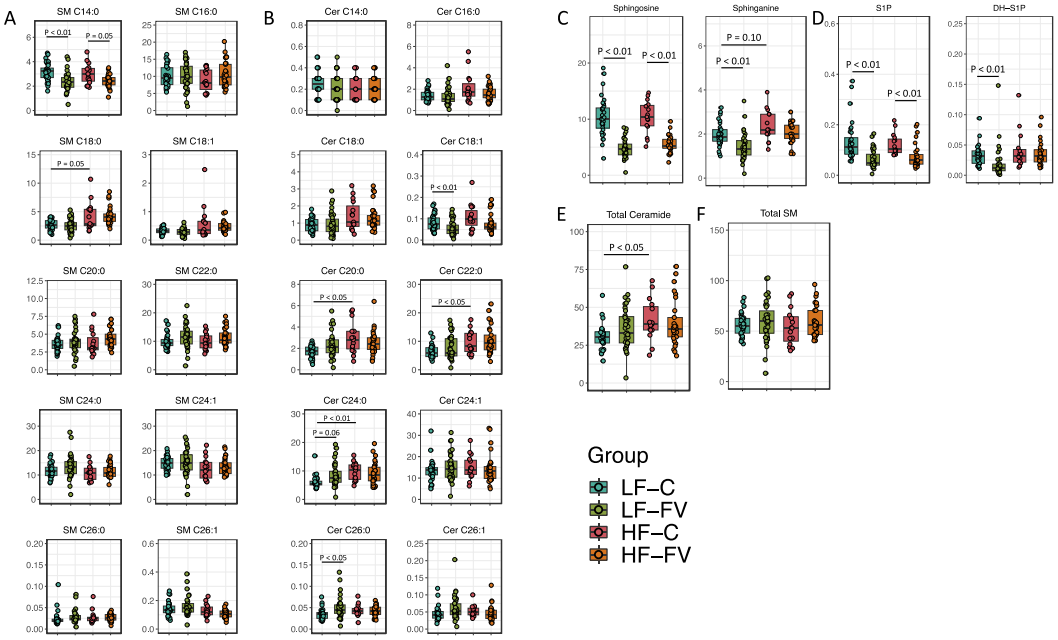

Panel 7: Levels of liver sphingomyelins, ceramides, and derivatives (pmoles/mg of tissue). F&V is associated with an overall reduction in liver sphingosine and S1P. Differences in concentrations of sphingolipids were determined using one-way ANOVA followed by Student's t-test and post-hoc adjustment for multiple comparisons. SM = sphingomyelin, Cer = ceramide, S1P = sphingosine-1-phosphate, DH-S1P = dihydro-S1P.

Because we observed an overall reduction in circulating SM's, and SM's can act as substrates for the generation of Cer and its associated products (i.e. sphingosine, sphinganine, S1P), we suspected that liver concentrations of Cer and species derivatives would be differentially abundant, which could affect liver cancer development. As shown in Figure 7A-B, only minor differences in liver SM and Cer were observed. In comparison to LF-C, HF-C had significantly higher levels of many Cer species, such as Cer C20:0, C22:0, and C24:0, as well as total Cer. No apparent effect of F&V was observed in liver SM or Cer, although, we note that on average different Cer species were lower in the HF-FV group in comparison to HF-C. Interestingly, we found that levels of sphingosine and S1P were both drastically reduced in the F&V supplemented groups in comparison to their non-supplemented counterparts. Unlike Cer, S1P is a pro-survival molecule. Further, sphinganine and dihydro-sphingosine-1-phosphate (DH-S1P) were lower in the LF-FV group in comparison to LF-C, whereas, in HF-FV mice, the levels of sphinganine and DH-S1P were lower on average in

comparison to HF-C, but not statistically different. Taken together, the circulating and liver sphingolipid data demonstrated that F&V supplementation was associated with a dramatic reduction in circulating SMs, which may be linked to the observed reduction of Cer derivatives such as sphingosine and S1P.

We next sought to: 1) determine how systemic cytokines, and both systemic and liver sphingolipids, were associated with one another, and 2) identify which features, across the 4 datasets, were associated with liver cancer.

Chapter 2: Omic-data integration reveals linkages among microbiome, sphingolipids, cytokines and liver cancer

We suspected that long-term feeding of mice with a HF-diet may predispose them to developing liver cancer due to pro-survival and anti-apoptotic environment (e.g. increased levels of IL-10, S1P). Additionally, our previous analysis in Chapter 1 identified microbiota associated with diet as well as liver cancer. To identify linkages across the 4 datasets, and to determine their association to liver cancer, we integrated the datasets using sparse projection to latent structures model for discriminant analysis (sPLS-DA) with the mixOmics R package. This systems biology approach may better model the underlying biology of complex disease conditions such as cancer.

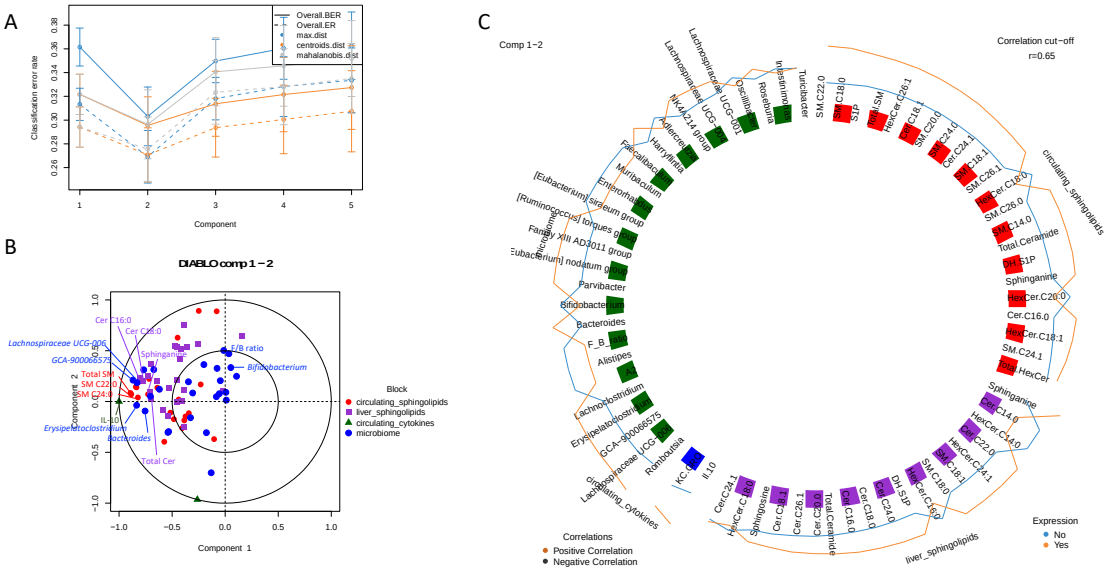

Panel 8: Multi-omic data integration reveals key linkages between the circulating cytokine, IL-10, and the gut microbiome and sphingolipids, according to liver cancer status. A) Classification error rate of sPLS-DA model, B) Correlation circle plot depicting overall correlation between the variable and the components, and C) Circos plot depicting correlations between the different variables. 'Expression' corresponds to presence (Yes) or absence (No) of liver cancer.

To prioritize the discriminative ability of our model we set the value for our design matrix to 0.1. For the initial multiblock sPLS-DA model we set the number of components at 5. When determining the ideal number of components for the final multiblock PLS-DA model we used the tuning function. As shown in Figure 8A, the ideal number of components was 2, as both the overall and balanced classification error rate increased with the addition of a 3rd, 4th, or 5th component. This observation was confirmed using the "choice.ncomp" function within the mixOmics R package. Selection of the number of features/variables from each data set to use for our final model was determined by using the "tune.block.splsda" function. The function was repeated a total of 30 times to increase our confidence in the selected number of variables. For the circulating sphingolipids block 18 and 5 species were selected for component 1 and 2, respectively. For the liver sphingolipids block 16 and 4 species were selected for component 1 and 2, respectively. For the microbiome block 10 and 18 genera were selected for component 1 and 2, respectively. Interestingly, for the cytokine block only 1 and 1 cytokines were selected for component 1 and 2, respectively. The loadings for components 1 and 2 are shown in SFig4A and B, respectively.

As shown in Figure 8B, we observe except for a handful of genera, that most of the microbiome variables were negatively correlated with the first component. The cytokine IL-10, and both liver and circulating sphingolipids were predominantly negatively correlated with the first component, similar to the microbiome variables. Interestingly, the variables that correlated most negatively with the first component were IL-10, total circulating SM, SM C22:0, SM C24:0, SM C26;1, SM C20:0, *GCA-900066575*, *Lachnospiraceae UCG-006*, *Erysipelatoclostridium*, and liver total Cer, sphinganine, Cer C16:0 and C18:0, features that were predominantly higher in the groups fed HF-diet, but in particular, those only fed HF-diet.

To visualize the strongest associations between the selected variables, we used a Circos plot (Figure 8C) with a correlation cut-off of 0.65. As demonstrated in Figure 8C many of the associations were positive and the levels of these variables were generally higher in mice with liver cancer, represented by the “Expression” levels around the Circos plot.

We found that IL-10 was strongly (association > 0.79) and positively correlated with total circulating SM, SM C18:0 SM C18:1, SM C20:0, SM C22:0, and SM C24:0. IL-10 was positively associated with total liver Cer levels and sphinganine, with the strongest correlation being with Cer C16:0 (association > 0.8) and Cer C18:0 (association > 0.77). Similarly, IL-10 was highly (association > 0.75) and positively linked to *GCA-900066575, Lachnoclostridium, Lachnospiraceae UCG-006,* and *Erysipelatoclostridium,* with the latter 4 having correlation coefficients above 0.8 and having been highly enriched in the microbiomes of HF-C mice. The *Bacteroides* genus was positively correlated with IL-10 (association = 0.76). Interestingly, the *Bacteroides* genus had strong positive associations (>0.66) with total circulating SM and SM C22:0. Further, it was positively associated with the other circulating SM species, with the lowest correlation coefficients being with SM C14:0 and SM C26:0, 0.46 and 0.47, respectively.
The positive association between the *Bacteroides* genus and SM pool is not surprising given that recent observations demonstrate that members of the Bacteroidetes phylum can not only produce sphingolipids but negatively affect host sphingolipid metabolism in mice fed HF diet.[117] Associations between sphingolipids and other microbiota were also uncovered. The microbiota *GCA-900066575, Lachnospiraceae UCG-006, and Erysipelatoclostridium* were the most strongly (association > 0.75) and positively associated with the SM pool, particularly with the total circulating SM, SM C18:0, C20:0, and C22:0. These genera were predominantly associated with the HF-C. In assessing associations between the liver sphingolipid pool and the microbiome, we found generally weaker associations than those observed above. Both *GCA-900066575* and *Lachnospiraceae UCG-006* were positively associated with liver Cer C16:0 and C18:0, with association coefficients ranging between 0.68-0.75.

Between the liver and circulating sphingolipid pools, we found that short-chain liver Cer C14:0, the levels of which were higher in mice without liver cancer, was positively correlated with total circulating Hex-Cer, Hex-Cer C18:0 and Hex-Cer C20:0. On the

other hand, liver Cer C16:0, Cer C18:1, and Cer C18:0, which were all elevated in mice with liver cancer, were all positively associated (>0.53) with total circulating SM, SM C18:1, SM C18:0, SM C20:0, SM C22:0, SM C24:1, SM C24:0, SM C26:1 and SM C26:0, which, as expected, suggests that levels of these liver Cer species are related to levels of circulating SM.

Taken together, the integration of our omic data sets demonstrated that key features, that were enriched predominantly in the HF-C group, could be used to discriminate mice with or without liver cancer, and thus further testing of these identified features is required to determine causality.

Chapter 3: Potential mechanisms

Towards determining the potential mechanisms and origins of the observed changes in sphingolipids and Il-10, and their link to the gut microbiome, we interrogated the expression of genes involved in sphingolipid metabolism and IL-10 in the liver, where the cancer was present, and in the colon, the tissue in immediate vicinity to the gut microbiome.

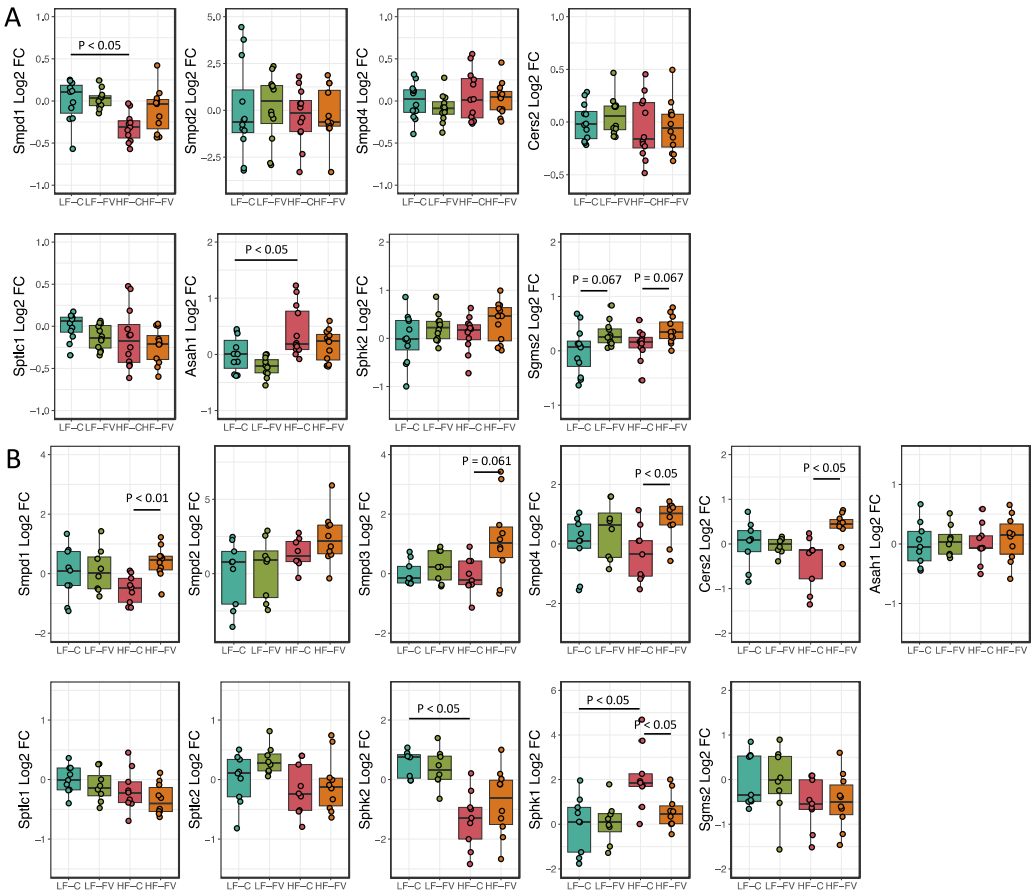

Panel 9: Expression of genes linked to sphingolipid metabolism in the liver (A) and proximal colon (B). For the liver, n = 11-12/group. For the proximal colon, n=7-9/group. The p-value shown has been adjusted for multiple comparisons using the Tukey method.

As shown in Figure 9A, a significant increase in the liver expression of the *Asah1* was observed in the HF-C group in comparison to LF-C. We found no differences in the expression of liver *Sptlc1* or *Cers2*, both of which encode proteins that participate in de novo ceramide synthesis. The expression of *Smpd1* (aSMase) was significantly reduced in the livers of HF-C mice in comparison to LF-C. No differences in the expression of liver *Smpd2* (nSMase1) or *4* (nSMase3). Importantly, higher levels of expression of *Asah1* have been previously linked to certain cancers as a way to reduce Cer levels.[131–133] Similarly, *Smpd1* activity has been consistently demonstrated to be triggered by TNF-α, and reduction in aSMase is one manner by which cancer cells can circumvent TNF-α induced apoptosis.[134]

Given that the gut microbiota and the circulating SM pool were strongly associated, we also assessed the expression of genes linked to sphingolipid metabolism in the proximal colon. The colon is the anatomical location in which the microbiome is densest and therefore most likely to directly affect host homeostasis. As shown in Figure 9B we found that in the proximal colon the expression of various SMase's was increased in the HF-FV group. Both *Smpd1* (aSMase) and *Smpd4* (nSMase3) were significantly increased in HF-FV mice in comparison to HF-C, and a similar trend was observed for *Smpd3* (nSMase2) and *Smpd2* (nSMase1), which were on average higher, but were statistically insignificant after adjustment for multiple comparisons. The expression levels of *Cers2* and *Sphk1* were also different in the HF-FV group in comparison to HF-C, with *Cers2* being expressed higher in HF-FV than HF-C, and with the level of *Sphk1* expression returning to LF-C levels. In LF-FV mice, the expression of *Smpd3* and *4* were on average higher than LF-C mice, but this was not statistically different. The expression of all other genes involved in sphingolipid metabolism in the colon were comparable between LF-C and LF-FV.

Taken together, HF-C mice have a gene expression profile that suggests they may have 1) increased capacity to convert Cer to sphingosine, and 2) impair Cer-induced apoptosis via the reduction in aSMase. These expression patterns could be adopted by cancerous cells to promote their survival. Notably, increased levels of S1P and Cer-1-P have been demonstrated to occur in many types of cancer in contrast to Cer and sphingosine.[135]

In the colon, the expression profiles of the HF-FV group are suggestive of having increased capacity to hydrolyze SM. However, because this was whole colonic tissue, we cannot determine the directionality (basolateral or apical) thus we cannot conclude whether the colon is digesting circulating SM or leftover dietary SM.

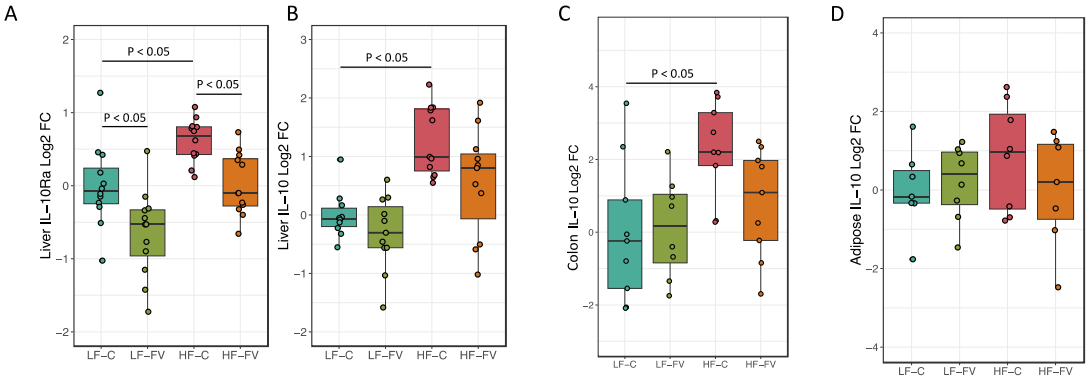

Panel 10: Expression of genes linked to IL-10 in the liver and proximal colon. A) Liver IL-10Ra expression, B) Liver IL-10 expression, C) colon IL-10 expression, and D) epididymal adipose IL-10 expression. For liver, n = 12/group; for proximal colon, n=9/group; for adipose, n = 8/group. The p-value shown has been adjusted for multiple comparisons using the Tukey method.

Given the strong linkage between IL-10 and liver cancer, we assessed the gene expression of *IL-10 receptor subunit a* (Ra). As demonstrated by Figure 10A, expression of *IL-10Ra* was significantly higher in HF-C mice, in comparison to both LF-C or HF-FV. Further, expression level of liver *IL-10* was approximately 2-fold higher in HF-C mice in comparison to LF-C (Figure 10B). Similarly, as shown in Figure 9C, the expression of colonic *IL-10* was 4-fold higher in the HF-C group in comparison to LF-C. Colonic expression of *IL-10* in HF-FV mice was approximately 50% lower than HF-C, but the difference was not significant. As shown in Figure 10D, no significant differences or trends were observed in *IL-10* gene expression in adipose tissue, although, on average, IL-10 expression was highest in the HF-C group. These data suggest that the colon and perhaps liver may be sources of circulating IL-10.

Discussion

In this thesis we sought to: 1) evaluate the gut microbiome at different life stages in mice that were supplemented with F&V, 2) determine how features of the gut microbiome, systemic inflammation, and sphingolipids, were associated with liver cancer, as well as 3) identifying an axis by which the gut microbiota could impact the development of cancer.

We found that age and diet were associated with unique gut microbiome compositions (as determined by β-diversity at the genera level). In agreement with previously reported observations, aging was associated with increasingly dissimilar microbiomes, as shown by the relative increase in Bray-Curtis values within groups across the different life stages. Furthermore, our data suggests that the overall composition of the gut microbiome was responsive to F&V supplementation, as demonstrated by the formation of distinct centroids, despite having similar base diets (LF- or HF-diet).

While we found that mice consuming a LF-diet had the most stable and least dissimilar microbiome compositions at 6 months of age, as demonstrated by the lowest mean Bray-Curtis dissimilarity values, the β-diversity values became widely disordered by the final time point (21 months), suggesting that the microbiomes of each mouse within the LF-C group become increasingly dissimilar with age despite continuous feeding of the same diet. These data support observations reported by others in which the gut microbiome becomes increasingly personalized with age. The increase in the inter-individual variability was mirrored across all the other groups but occurred sooner (~6 months). This is likely because all mice were fed LF-diet during the acclimatization phase and prior to randomization (about 2-3 weeks total). This result suggests that the gut microbiome composition was quickly established (within 2-3 weeks of LF-diet feeding), since the β-diversity/dissimilarity values of the LF-C group were not substantially higher going from 0 to 6 months of age. In the LF-FV group, the gut microbiomes were relatively stable from 6-21 months of age, suggesting that once the gut microbiomes of LF-FV mice were established they remained relatively stable throughout the mouse's lifespan. A similar observation was made for HF-C and HF-FV. We also demonstrated that F&V was associated with a higher F/B ratio at the end of the study, a feature of the microbiome that is typically reduced with age due to loss of Firmicutes. In our study, maintenance of the F/B ratio appears to be due to an expansion of the Firmicutes. In our mixed effects regression model, we found that age affected the F/B ratio ($P < 0.001$) as did the interaction between diet and age ($P < 0.05$). Diet by itself did not significantly affect the F/B ratio but was close to significance ($P = 0.104$). Surprisingly, in our model age alone was positively and significantly associated with F/B ratio, however, the directionality of the diet and age interaction term depended on the type of diet. The coefficient for the HF-C*age interaction term was negative while the HF-FV*age interaction term was positive indicating that feeding HF-diet alone with

increasing age was associated with a decreasing F/B ratio, while F&V supplementation appears to partially rescue this effect. Thus, F/B ratio depends on both age and its interaction with diet. This corroborates our earlier PERMANOVA results which demonstrated that age alone could explain the variation in the β diversity values ($P<0.001$), while diet alone could not ($P = 1$). However, when combining diet and age, the PERMANOVA revealed a significant effect of diet. Thus, our analysis suggests that the F/B ratio and general microbiome composition is highly dependent on age, but diet patterns can have a significant impact with increasing age. This observation is relevant for studies that aim to leverage the F/B as a marker of gut microbiome health and may explain the observed variability across different study populations.[136,137]

In our longitudinal analysis, age was strongly associated with an enrichment of *Faecalibaculum, Ileibacterium, Roseburia,* and *Bifidobacterium*, *Lachnospiraceae NK4A136*, and *Colidextribater*. Conversely, age was associated with a robust reduction in *Lactobacillus, UCG-005, Akkermansia,* and *Marvinbryantia*, among others. Importantly, despite MassLin2 reporting an age-associated enrichment of these bacteria, we do note that some of these bacteria, such as *Bifidobacterium,* were not enriched in all the groups with age. Our longitudinal analysis indicated that *Bifidobacterium* was higher in LF-FV in comparison to LF-C, while in the HF-C group the levels of *Bifidobacterium* were comparable to LF-C. Further, in the HF-FV group, the levels of *Bifidobacterium* were lower in comparison to HF-C. *Streptococcus* was positively associated with age, HF-C was the group with the highest levels. Inspection of the TSS values for *Streptococcus* did reveal an increase in the levels of this bacteria across all groups but was most robust in the HF-C group. Thus, in some cases, age-associated changes reported by Masslin2 are likely to be driven by specific group changes and should be interpreted with caution, future analysis should assess potential diet and age interactions longitudinally.

Our longitudinal analysis also demonstrated that each diet was associated with its own differentially abundant genera. Importantly, we report that only the HF-C group was longitudinally associated with an enrichment of the *Streptococcus* and *Enterococcus* genera, both of which have been previously associated with liver cancer in cross-sectional studies.[127,138,139] Other taxa such as *[Eubacterium] nodatum group*, *Erysipelatoclostridium, Tuzzerella,* and *[Ruminococcus] torques group*, were also

increased in only the HF-C group. F&V supplementation, in the background of HF-diet, attenuated the increase in these genera. In our study, *[Ruminococcus] torques group, and Romboutsia,* were positively and significantly associated with liver cancer, and other studies have similarly linked the presence of these genera to liver cancer.[77] While not significant, after adjusting for multiple hypothesis testing, *Streptococcus* was also positively associated with liver cancer and trended towards significance (P = 0.09). Conversely, the level of the *Bifidobacterium* genera was negatively associated with liver cancer. Levels of Bifidobacterium were highest in the LF-FV group in comparison to LF-C, while no differences in *Bifidobacterium* were found between HF-C and LF-C. However, levels of *Bifidobacterium* were modestly different between HF-C and HF-FV, with the levels of *Bifidobacterium* being modestly higher in the HF-C group. Thus, it may be a unique combination of microbiota that may directly increase the risk of liver cancer in the HF-C group.

In both F&V supplemented groups, microbiome changes were associated with an increase in SCFA-producing bacteria, such as *Lachnospiraceae NK4A136* and *ASF356.* Quantitation of SCFA's confirmed that at the end of the study, fecal SCFA levels of butyric and acetic acid were significantly higher in the F&V supplemented groups. Propionic acid was significantly higher only in the LF-FV group. Correlation analysis between diet-associated microbiota and SCFAs revealed that F&V-associated microbiota such as *Lachnospiraceae NK4A136*, *ASF356, Acetatifactor, Lachnospiraceae UCG-001 and UCG-009,* were significantly and highly correlated with levels of butyric and acetic acid, and in some cases propionic acid as well.

We subsequently found that circulating levels of total SM and some specific SM species were substantially lower in the F&V supplemented mice. Additionally, total circulating Cer and some Cer species were reduced in LF-FV, but not HF-FV. In the liver we demonstrated that total Cer and specific Cer species were elevated in HF-C mice in comparison to LF-C. We observed a reduction in the levels of sphingosine and S1P in both F&V treated groups. F&V supplementation significantly reduced the levels of sphinganine only in LF-fed mice, and not HF-fed mice. Further, we demonstrate that F&V reduced the levels of pro-inflammatory cytokines, TNF-α and IL-6, anti-inflammatory cytokine, IL-10, and chemokines, MCP-1 and KC-GRO, in LF-fed mice. However, in HF-fed mice receiving F&V supplementation, the levels of IL-6 and IL-10 were lower on

average in comparison to HF-C but the differences were not statistically significant. Notably, when comparing HF-C vs LF-C, we found a significant difference in circulating IL-10, which was approximately 2-fold higher in HF-C mice compared to LF-C. Levels of IL-10 have been demonstrated to acutely increase with HF-diet feeding and are suggested to be an adaptive mechanism that can protect against diet-induced insulin resistance in the liver[140] and delivery of IL-10 can attenuate diet-induced obesity.[141] Individuals with low levels of IL-10 are also associated with obesity and metabolic syndrome,[142] suggesting that IL-10 is a critical protective factor against obesity. Higher levels of circulating IL-10 concomitant with an enrichment of pathogenic genera, *Enterobacter* and *Enterococcus,* in patients with non-alcoholic fatty liver, was recently reported.[138] These observations suggest that features commonly observed in human studies of liver disease may be recapitulated in mouse models of aging.

Integration of our 4-omic data sets at the final time point revealed novel associations between microbiota, sphingolipids and IL-10, as well as demonstrated that the features predominantly enriched or present in HF-C mice were the best at discriminating liver cancer status. Interestingly, circulating IL-10 was found to be strongly and positively associated with HF-diet associated microbiota, circulating SM's, liver sphinganine, and Cer C16:0 and C18:0. This analysis suggests that the combination of these features can drive the development of liver cancer and importantly, reflect key processes that may be hijacked by cancerous cells to promote their survival. The strong linkages between IL-10 and the other markers suggest that IL-10 is important for the development of HF-diet associated liver cancer. We speculate that IL-10 increase is an acute adaptive response meant to counteract the effects of HF-diet, however, chronic HF-diet feeding may lead to chronic secretion of IL-10 which may promote an immunosuppressive environment and facilitate immune surveillance mechanisms.

We also sought to identify how differences in the expression of genes involved in sphingolipid metabolism could be altered to promote liver cancer, particularly those involved in SM synthesis and Cer-induced apoptosis. Investigation of liver expression of genes linked to ceramide metabolism revealed a significant reduction in aSMase (*Smpd1*) in the livers of HF-C mice. *Smpd1* is the predominant SMase expressed in the liver. aSMase converts SM to Cer in the lysosome, and its activity has been reported to be inducible by TNF-α.[143] By reducing the expression of aSMase, HF-C mice may

circumvent TNF-α induced apoptosis, since increased activity of aSMase can increase levels of Cer to promote pro-apoptotic pathways.[144] Exogenous provision of SM has been demonstrated to promote apoptosis via the generation of Cer.[145] While Cer mechanisms can contribute to metabolic diseases, and reducing the level of Cer improves insulin sensitivity;[146] in the context of aging and cancer, Cer, via its pro-apoptotic properties is a tumor-suppressor lipid which induces an antiproliferative and pro-apoptotic response in various cancer cells.[147] In fact, inhibition of ceramidase (*Asah*) sensitizes hepatoma cells to chemotherapy and reduces tumor growth *in vivo.*[148] Similarly, we also found a modest difference in the expression *Asah1* in HF-C mice in comparison to LF-C. Increased *Asah1*, may reflect the ability to circumvent increases in Cer levels by rapidly converting it to sphingosine and subsequently S1P, a pro-survival Cer species. In our mouse model, it appears that HF diet, in the absence of F&V, promotes changes in gene expression in sphingolipid metabolism that promote survival and growth, an observation in-agreement with previous observations in human and *in vitro* cancer studies.

When determining potential sources of IL-10 we checked the gene expression of IL-10 in the liver and colon. We found a 2-fold increase in the expression of IL-10 in the liver. Further, we found that IL-10 expression was 4-fold higher in the colon. Given the importance of IL-10 for colon homeostasis,[149] we ponder whether colonic-derived IL-10 can appreciably contribute to circulating levels of IL-10. No significant differences in IL-10 expression were observed in epididymal adipose tissue, however, IL-10 could arise from other adipose depots. Additionally, we observed higher levels of expression of liver *IL-10Ra* in the HF-C group. IL-10 can both inhibit LPS-induced NF-κB activation to prevent TNF-α production[150] and can inhibit TNF-α-induced apoptosis. Furthermore, higher co-expression of IL-10 and IL-10 receptor have been observed in tumors.[151] Given that targeted cell death, via TNF-α, is one of the key methods by which to maintain the tissue homeostasis and clearance of deleterious cells,[152] increasing IL-10 and S1P levels concomitant with a reduction in aSMase may theoretically create an environment that is more permissive to cancer cell survival, proliferation and angiogenesis. Studies have previously correlated levels of tumor-produced IL-10 with their ability to cause immunosuppression.[153,154] Interestingly, a recent study (pre-print) demonstrated that IL-10 signaling can also constrain sphingolipid metabolism, particular production of long-chain Cer's.[155] This suggests that IL-10 and sphingolipid metabolism

may work in conjunction. Taken together these data suggest that HF-diet alone may promote a pro-survival and immunosuppressive environment by circumventing pro-apoptotic mechanisms and promoting IL-10 production.

Given the strong negative linkage between circulating SM's and the gut microbiome, we also assessed the expression pattern of genes linked to sphingolipid metabolism in the proximal colon, which we hoped would illuminate the potential contributions of the microbiome to the host sphingolipidome. Analysis of the expression of genes linked to sphingolipid metabolism in the proximal colon revealed increased expression of aSMase (*Smpd1*), nSMase3 (*Smpd4*) and Cers2 in the HF-FV group in comparison to HF-C. While not significant, the expression of nSMase1 (*Smpd2*) and nSMase2 (*Smpd3*) was on average higher in the HF-FV group in comparison to HF-C. Suggesting that the colon is increasing its hydrolysis of SM and synthesis of Cer via Cers2. While statistically insignificant, the expression of *Smpd3* and *Smpd4* were on average higher in the LF-FV group in comparison to the LF-C group, of note, *Smpd3* is the SMase most expressed in the colon. Increased expression of colon SMase suggests increased colonic hydrolysis of SM. However, because this was whole colonic tissue, we cannot determine we cannot conclude if the colon is digesting dietary SM. Interestingly, HF-diet feeding has been demonstrated to reduce alkaline SMase.[156] however, we could not measure the expression of genes involved in sphingolipid metabolism in the small intestine, which is where digestion and metabolism of SM predominantly occurs.[157] Neither did we measure the expression of genes involved in sphingolipid metabolism in adipose tissue. While not significant after adjustment, we observed an increase in the level of expression of genes involved in SM synthesis (*Sgms2*) in both F&V supplemented groups. This increased expression was surprising given that we observed higher levels of circulating SM in non-supplemented groups. We would expect that both HF-diet fed groups to have similar levels of sphingolipids given that the predominant source of sphingolipids in mouse diets should come from fat,[158] yet we found significant differences in sphingolipid profiles between HF-C vs HF-FV. Future studies should address the source of circulating SM and sphingolipid digestion/absorption in the small intestine.

The data put forth herein suggests that F&V supplementation is associated with favorable changes in microbiome, sphingolipidome, and systemic inflammatory milieu. Further, it suggests that lifelong HF-diet feeding is associated with high levels of

circulating IL-10, liver Cer, and liver expression of *Asah1, IL-10,* and *IL-10Ra*, concomitant with a reduction in the expression of liver *Smpd1* (aSMase). These changes may favor cancer cell survival and suppress immune surveillance mechanisms. Interestingly, we observed that both LF-C and HF-C mice were associated with increased circulating SM and liver S1P and sphingosine, yet liver *Sgms2* expression was modestly decreased in both groups. Conversely, we found that LF-FV and HF-FV had reduced levels of these same factors. Thus, we are left to speculate why circulating SM levels are similar between LF-C and HF-C, given that HF-diet fed mice should have higher levels of dietary intake of sphingolipids. One potential source could be the microbiota, such as members of the Bacteroidetes phylum. We do note that the *Bacteroides* genus was positively associated with total circulating SM, SM C22:0, SM C18:0, SM C20:0, and SM C26:1 (association coefficient > 0.6). Thus, it is plausible that F&V-associated changes in the prevalence of the *Bacteroides*, and other members of the Bacteroidetes phylum, could mediate the reduction in circulating SM's. F&V may favor the colonization of members of the Firmicutes phylum, which may negatively interact with members of the Bacteroidetes phylum, and it is through this process that F&V may protect mice despite HF-diet feeding. However, an alternative avenue could be linked to the increased hydrolysis of SM in the colon. HF-FV mice had increased expression of SMase's which may reduce the level circulating SM in comparison to HF-C mice. Further, a study performed in 1996 demonstrated that bacteria were associated with enhanced alkaline SMase activity as the activity in the intestinal mucosa of bacteria-free mice was lower than samples with bacteria.[159] Thus, future studies should determine the source of SM and the role of the microbiota in affecting host-sphingolipid metabolism.

It is important to note the limitations of this study. The experiments and data analyses presented herein arose from a longitudinal study that sought to determine differences in median lifespan and healthspan. To identify potential mechanisms, the secondary outcomes collected were microbiome, systemic cytokines, and liver and circulating sphingolipids. In this study the HF-C group was the first to reach median lifespan. Upon sacrificing the mice, we had observed that a significant portion of the mice in the HF-C group had liver cancer. Only 2 mice were found to have no cancerous lesions. Thus, we could not perform univariate analyses within groups to determine if differences in the secondary outcomes differed between mice with or without liver cancer. Nevertheless,

assessment of putative markers (i.e. inflammation, sphingolipids, microbiome) of health and disease and their multi-omic integration has illuminated a potential axis by which F&V may mitigate liver cancer risk. Many of our observations are in-agreement with observations made by others in different models and studies of cancer. Here demonstrate that lifelong F&V supplementation can attenuate the enrichment of diet- and age-associated potentially harmful genera (i.e. *Streptococcus)*, promote a higher F/B ratio, increase SCFA levels, and promote favorable changes in the host sphingolipidome and inflammatory milieu. We identify specific gene signatures which may also be altered in obesity settings, and which are responsive to F&V supplementation. Future research is warranted to determine the role of HF-diet or HF-diet-associated microbiota or sphingolipids and their strong association with systemic levels of IL-10. Furthermore, analysis of other organs/tissues that contribute to IL-10 secretion and sphingolipid metabolism should be characterized. Finally, the markers identified here via our supervised sPLS-DA model should be tested in another human or mouse dataset for further validation.

Bibliography/References

1. Crimmins, E. M. Lifespan and Healthspan: Past, Present, and Promise. *Gerontologist* **55**, 901–911 (2015).
2. Dong, X., Milholland, B. & Vijg, J. Evidence for a limit to human lifespan. *Nature* **538**, 257–259 (2016).
3. Garmany, A., Yamada, S. & Terzic, A. Longevity leap: mind the healthspan gap. *NPJ Regen Med* **6**, 57 (2021).
4. Kolovou, G. D., Kolovou, V. & Mavrogeni, S. We are ageing. *Biomed Res. Int.* **2014**, 808307 (2014).
5. Wang, X. *et al.* Fruit and vegetable consumption and mortality from all causes, cardiovascular disease, and cancer: systematic review and dose-response meta-analysis of prospective cohort studies. *BMJ* **349**, g4490 (2014).
6. Lieberman, D. E., Kistner, T. M., Richard, D., Lee, I.-M. & Baggish, A. L. The active

grandparent hypothesis: Physical activity and the evolution of extended human healthspans and lifespans. *Proc. Natl. Acad. Sci. U. S. A.* **118**, (2021).

7. Hou, K. *et al.* Microbiota in health and diseases. *Signal Transduct Target Ther* **7**, 135 (2022).
8. Larson, P. J. *et al.* Associations of the skin, oral and gut microbiome with aging, frailty and infection risk reservoirs in older adults. *Nat Aging* **2**, 941–955 (2022).
9. Claesson, M. J. *et al.* Gut microbiota composition correlates with diet and health in the elderly. *Nature* **488**, 178–184 (2012).
10. Moreno-Indias, I. *et al.* Red wine polyphenols modulate fecal microbiota and reduce markers of the metabolic syndrome in obese patients. *Food Funct.* **7**, 1775–1787 (2016).
11. Guo, W. *et al.* Long-term supplementation with fruits and vegetables prolongs lifespan and reduces tumor incidence in mice fed a western-style high-fat diet. *Curr. Dev. Nutr.* **6**, 6009022 (2022).
12. Guo, W. *et al.* A Novel Combination of Fruits and Vegetables Prevents Diet-Induced Hepatic Steatosis and Metabolic Dysfunction in Mice. *J. Nutr.* **150**, 2950–2960 (2020).
13. López-Otín, C., Blasco, M. A., Partridge, L., Serrano, M. & Kroemer, G. The hallmarks of aging. *Cell* **153**, 1194–1217 (2013).
14. Picco, L. *et al.* Economic burden of multimorbidity among older adults: impact on healthcare and societal costs. *BMC Health Serv. Res.* **16**, 173 (2016).
15. Salive, M. E. Multimorbidity in older adults. *Epidemiol. Rev.* **35**, 75–83 (2013).
16. Salvestrini, V., Sell, C. & Lorenzini, A. Obesity May Accelerate the Aging Process. *Front. Endocrinol.* **10**, 266 (2019).
17. Zmora, N., Suez, J. & Elinav, E. You are what you eat: diet, health and the gut microbiota. *Nat. Rev. Gastroenterol. Hepatol.* **16**, 35–56 (2019).

18. Koponen, K. K. *et al.* Associations of healthy food choices with gut microbiota profiles. *Am. J. Clin. Nutr.* **114**, 605–616 (2021).
19. Sanders, M. E., Merenstein, D. J., Reid, G., Gibson, G. R. & Rastall, R. A. Probiotics and prebiotics in intestinal health and disease: from biology to the clinic. *Nat. Rev. Gastroenterol. Hepatol.* **16**, 605–616 (2019).
20. Fogliano, V. *et al.* In vitro bioaccessibility and gut biotransformation of polyphenols present in the water-insoluble cocoa fraction. *Mol. Nutr. Food Res.* **55 Suppl 1**, S44–55 (2011).
21. Wang, S. *et al.* Gut microbiota mediates the anti-obesity effect of calorie restriction in mice. *Sci. Rep.* **8**, 13037 (2018).
22. Ruppin, H., Bar-Meir, S., Soergel, K. H., Wood, C. M. & Schmitt, M. G., Jr. Absorption of short-chain fatty acids by the colon. *Gastroenterology* **78**, 1500–1507 (1980).
23. Macfarlane, S. & Macfarlane, G. T. Regulation of short-chain fatty acid production. *Proc. Nutr. Soc.* **62**, 67–72 (2003).
24. Roediger, W. E. Role of anaerobic bacteria in the metabolic welfare of the colonic mucosa in man. *Gut* **21**, 793–798 (1980).
25. Rechkemmer, G., Rönnau, K. & von Engelhardt, W. Fermentation of polysaccharides and absorption of short chain fatty acids in the mammalian hindgut. *Comp. Biochem. Physiol. A Comp. Physiol.* **90**, 563–568 (1988).
26. Segain, J. P. *et al.* Butyrate inhibits inflammatory responses through NFkappaB inhibition: implications for Crohn's disease. *Gut* **47**, 397–403 (2000).
27. Atarashi, K. *et al.* Treg induction by a rationally selected mixture of Clostridia strains from the human microbiota. *Nature* **500**, 232–236 (2013).
28. Furusawa, Y. *et al.* Commensal microbe-derived butyrate induces the differentiation of colonic regulatory T cells. *Nature* **504**, 446–450 (2013).

29. Kashiwagi, I. *et al.* Smad2 and Smad3 Inversely Regulate TGF-β Autoinduction in Clostridium butyricum-Activated Dendritic Cells. *Immunity* **43**, 65–79 (2015).
30. Chang, P. V., Hao, L., Offermanns, S. & Medzhitov, R. The microbial metabolite butyrate regulates intestinal macrophage function via histone deacetylase inhibition. *Proc. Natl. Acad. Sci. U. S. A.* **111**, 2247–2252 (2014).
31. Maslowski, K. M. *et al.* Regulation of inflammatory responses by gut microbiota and chemoattractant receptor GPR43. *Nature* **461**, 1282–1286 (2009).
32. Wu, W. *et al.* Microbiota metabolite short-chain fatty acid acetate promotes intestinal IgA response to microbiota which is mediated by GPR43. *Mucosal Immunol.* **10**, 946–956 (2017).
33. Tong, L.-C. *et al.* Propionate Ameliorates Dextran Sodium Sulfate-Induced Colitis by Improving Intestinal Barrier Function and Reducing Inflammation and Oxidative Stress. *Front. Pharmacol.* **7**, 253 (2016).
34. Ma, X. *et al.* Butyrate promotes the recovering of intestinal wound healing through its positive effect on the tight junctions. *J. Anim. Sci.* **90 Suppl 4**, 266–268 (2012).
35. Tolhurst, G. *et al.* Short-chain fatty acids stimulate glucagon-like peptide-1 secretion via the G-protein-coupled receptor FFAR2. *Diabetes* **61**, 364–371 (2012).
36. Frost, G. *et al.* The short-chain fatty acid acetate reduces appetite via a central homeostatic mechanism. *Nat. Commun.* **5**, 3611 (2014).
37. Cummings, J. H., Pomare, E. W., Branch, W. J., Naylor, C. P. & Macfarlane, G. T. Short chain fatty acids in human large intestine, portal, hepatic and venous blood. *Gut* **28**, 1221–1227 (1987).
38. Canfora, E. E. *et al.* Colonic infusions of short-chain fatty acid mixtures promote energy metabolism in overweight/obese men: a randomized crossover trial. *Sci. Rep.* **7**, 2360 (2017).
39. Chambers, E. S. *et al.* Acute oral sodium propionate supplementation raises resting

energy expenditure and lipid oxidation in fasted humans. *Diabetes Obes. Metab.* **20**, 1034–1039 (2018).

40. Xiong, Y. *et al.* Short-chain fatty acids stimulate leptin production in adipocytes through the G protein-coupled receptor GPR41. *Proc. Natl. Acad. Sci. U. S. A.* **101**, 1045–1050 (2004).
41. Liu, R. H. Health benefits of fruit and vegetables are from additive and synergistic combinations of phytochemicals. *Am. J. Clin. Nutr.* **78**, 517S–520S (2003).
42. Clifford, M. N. Diet-derived phenols in plasma and tissues and their implications for health. *Planta Med.* **70**, 1103–1114 (2004).
43. Vanegas, S. M. *et al.* Substituting whole grains for refined grains in a 6-wk randomized trial has a modest effect on gut microbiota and immune and inflammatory markers of healthy adults. *Am. J. Clin. Nutr.* **105**, 635–650 (2017).
44. Singh, D. P. *et al.* Co-supplementation of isomalto-oligosaccharides potentiates metabolic health benefits of polyphenol-rich cranberry extract in high fat diet-fed mice via enhanced gut butyrate production. *Eur. J. Nutr.* **57**, 2897–2911 (2018).
45. Fava, F. & Danese, S. Intestinal microbiota in inflammatory bowel disease: friend of foe? *World J. Gastroenterol.* **17**, 557–566 (2011).
46. Aldars-García, L., Chaparro, M. & Gisbert, J. P. Systematic Review: The Gut Microbiome and Its Potential Clinical Application in Inflammatory Bowel Disease. *Microorganisms* **9**, (2021).
47. Lo Presti, A. *et al.* Fecal and Mucosal Microbiota Profiling in Irritable Bowel Syndrome and Inflammatory Bowel Disease. *Front. Microbiol.* **10**, 1655 (2019).
48. Sankarasubramanian, J., Ahmad, R., Avuthu, N., Singh, A. B. & Guda, C. Gut Microbiota and Metabolic Specificity in Ulcerative Colitis and Crohn's Disease. *Front. Med.* **7**, 606298 (2020).
49. Bäckhed, F. *et al.* The gut microbiota as an environmental factor that regulates fat

storage. *Proc. Natl. Acad. Sci. U. S. A.* **101**, 15718–15723 (2004).

50. Li, W.-Z., Stirling, K., Yang, J.-J. & Zhang, L. Gut microbiota and diabetes: From correlation to causality and mechanism. *World J. Diabetes* **11**, 293–308 (2020).
51. Fang, P., Kazmi, S. A., Jameson, K. G. & Hsiao, E. Y. The Microbiome as a Modifier of Neurodegenerative Disease Risk. *Cell Host Microbe* **28**, 201–222 (2020).
52. Yu, L.-X. & Schwabe, R. F. The gut microbiome and liver cancer: mechanisms and clinical translation. *Nat. Rev. Gastroenterol. Hepatol.* **14**, 527–539 (2017).
53. Cani, P. D. *et al.* Changes in gut microbiota control metabolic endotoxemia-induced inflammation in high-fat diet-induced obesity and diabetes in mice. *Diabetes* **57**, 1470–1481 (2008).
54. Ley, R. E. *et al.* Obesity alters gut microbial ecology. *Proc. Natl. Acad. Sci. U. S. A.* **102**, 11070–11075 (2005).
55. Collado, M. C., Isolauri, E., Laitinen, K. & Salminen, S. Distinct composition of gut microbiota during pregnancy in overweight and normal-weight women. *Am. J. Clin. Nutr.* **88**, 894–899 (2008).
56. Waldram, A. *et al.* Top-down systems biology modeling of host metabotype-microbiome associations in obese rodents. *J. Proteome Res.* **8**, 2361–2375 (2009).
57. Santacruz, A. *et al.* Gut microbiota composition is associated with body weight, weight gain and biochemical parameters in pregnant women. *Br. J. Nutr.* **104**, 83–92 (2010).
58. Da Silva, C. C., Monteil, M. A. & Davis, E. M. Overweight and Obesity in Children Are Associated with an Abundance of Firmicutes and Reduction of Bifidobacterium in Their Gastrointestinal Microbiota. *Child. Obes.* **16**, 204–210 (2020).
59. Cani, P. D. *et al.* Selective increases of bifidobacteria in gut microflora improve high-fat-diet-induced diabetes in mice through a mechanism associated with endotoxaemia. *Diabetologia* **50**, 2374–2383 (2007).

60. Schellekens, H. *et al.* Bifidobacterium longum counters the effects of obesity: Partial successful translation from rodent to human. *EBioMedicine* **63**, 103176 (2021).
61. Falony, G., Vlachou, A., Verbrugghe, K. & De Vuyst, L. Cross-feeding between Bifidobacterium longum BB536 and acetate-converting, butyrate-producing colon bacteria during growth on oligofructose. *Appl. Environ. Microbiol.* **72**, 7835–7841 (2006).
62. Paik, J. M., Golabi, P., Younossi, Y., Mishra, A. & Younossi, Z. M. Changes in the Global Burden of Chronic Liver Diseases From 2012 to 2017: The Growing Impact of NAFLD. *Hepatology* **72**, 1605–1616 (2020).
63. Tilg, H., Cani, P. D. & Mayer, E. A. Gut microbiome and liver diseases. *Gut* **65**, 2035–2044 (2016).
64. Michelotti, G. A., Machado, M. V. & Diehl, A. M. NAFLD, NASH and liver cancer. *Nat. Rev. Gastroenterol. Hepatol.* **10**, 656–665 (2013).
65. Shen, F. *et al.* Gut microbiota dysbiosis in patients with non-alcoholic fatty liver disease. *Hepatobiliary Pancreat. Dis. Int* **16**, 375–381 (2017).
66. Lopez-Siles, M., Duncan, S. H., Garcia-Gil, L. J. & Martinez-Medina, M. Faecalibacterium prausnitzii: from microbiology to diagnostics and prognostics. *ISME J.* **11**, 841–852 (2017).
67. Miquel, S. *et al.* Identification of metabolic signatures linked to anti-inflammatory effects of Faecalibacterium prausnitzii. *MBio* **6**, (2015).
68. Aron-Wisnewsky, J. *et al.* Gut microbiota and human NAFLD: disentangling microbial signatures from metabolic disorders. *Nat. Rev. Gastroenterol. Hepatol.* **17**, 279–297 (2020).
69. Le Roy, T. *et al.* Intestinal microbiota determines development of non-alcoholic fatty liver disease in mice. *Gut* **62**, 1787–1794 (2013).
70. Chiu, C.-C. *et al.* Nonalcoholic Fatty Liver Disease Is Exacerbated in High-Fat Diet-

Fed Gnotobiotic Mice by Colonization with the Gut Microbiota from Patients with Nonalcoholic Steatohepatitis. *Nutrients* **9**, (2017).

71. Hoyles, L. *et al.* Molecular phenomics and metagenomics of hepatic steatosis in non-diabetic obese women. *Nat. Med.* **24**, 1070–1080 (2018).
72. Sayin, S. I. *et al.* Gut microbiota regulates bile acid metabolism by reducing the levels of tauro-beta-muricholic acid, a naturally occurring FXR antagonist. *Cell Metab.* **17**, 225–235 (2013).
73. Kakiyama, G. *et al.* Modulation of the fecal bile acid profile by gut microbiota in cirrhosis. *J. Hepatol.* **58**, 949–955 (2013).
74. Daubioul, C. A., Horsmans, Y., Lambert, P., Danse, E. & Delzenne, N. M. Effects of oligofructose on glucose and lipid metabolism in patients with nonalcoholic steatohepatitis: results of a pilot study. *Eur. J. Clin. Nutr.* **59**, 723–726 (2005).
75. Demigné, C. *et al.* Effect of propionate on fatty acid and cholesterol synthesis and on acetate metabolism in isolated rat hepatocytes. *Br. J. Nutr.* **74**, 209–219 (1995).
76. Malaguarnera, M. *et al.* Bifidobacterium longum with fructo-oligosaccharides in patients with non alcoholic steatohepatitis. *Dig. Dis. Sci.* **57**, 545–553 (2012).
77. Komiyama, S. *et al.* Profiling of tumour-associated microbiota in human hepatocellular carcinoma. *Sci. Rep.* **11**, 10589 (2021).
78. Bindels, L. B. *et al.* Gut microbiota-derived propionate reduces cancer cell proliferation in the liver. *Br. J. Cancer* **107**, 1337–1344 (2012).
79. Siavoshian, S. *et al.* Butyrate and trichostatin A effects on the proliferation/differentiation of human intestinal epithelial cells: induction of cyclin D3 and p21 expression. *Gut* **46**, 507–514 (2000).
80. Smith, P. *et al.* Regulation of life span by the gut microbiota in the short-lived African turquoise killifish. *Elife* **6**, (2017).
81. Biagi, E. *et al.* Gut Microbiota and Extreme Longevity. *Curr. Biol.* **26**, 1480–1485

(2016).

82. Wang, F. *et al.* Gut Microbiota Community and Its Assembly Associated with Age and Diet in Chinese Centenarians. *J. Microbiol. Biotechnol.* **25**, 1195–1204 (2015).
83. Biagi, E. *et al.* Through ageing, and beyond: gut microbiota and inflammatory status in seniors and centenarians. *PLoS One* **5**, e10667 (2010).
84. Claesson, M. J. *et al.* Composition, variability, and temporal stability of the intestinal microbiota of the elderly. *Proc. Natl. Acad. Sci. U. S. A.* **108 Suppl 1**, 4586–4591 (2011).
85. Mariat, D. *et al.* The Firmicutes/Bacteroidetes ratio of the human microbiota changes with age. *BMC Microbiol.* **9**, 123 (2009).
86. Li, W. & Ma, Z. S. FBA Ecological Guild: Trio of Firmicutes-Bacteroidetes Alliance against Actinobacteria in Human Oral Microbiome. *Sci. Rep.* **10**, 287 (2020).
87. Langille, M. G. *et al.* Microbial shifts in the aging mouse gut. *Microbiome* **2**, 50 (2014).
88. Trayssac, M., Hannun, Y. A. & Obeid, L. M. Role of sphingolipids in senescence: implication in aging and age-related diseases. *J. Clin. Invest.* **128**, 2702–2712 (2018).
89. Li, S. & Kim, H.-E. Implications of Sphingolipids on Aging and Age-Related Diseases. *Front Aging* **2**, 797320 (2021).
90. Green, C. D., Maceyka, M., Cowart, L. A. & Spiegel, S. Sphingolipids in metabolic disease: The good, the bad, and the unknown. *Cell Metab.* **33**, 1293–1306 (2021).
91. Chaurasia, B. & Summers, S. A. Ceramides in Metabolism: Key Lipotoxic Players. *Annu. Rev. Physiol.* **83**, 303–330 (2021).
92. Lucki, N. C. & Sewer, M. B. Nuclear sphingolipid metabolism. *Annu. Rev. Physiol.* **74**, 131–151 (2012).
93. Maceyka, M., Payne, S. G., Milstien, S. & Spiegel, S. Sphingosine kinase,

sphingosine-1-phosphate, and apoptosis. *Biochim. Biophys. Acta* **1585**, 193–201 (2002).

94. Airola, M. V. & Hannun, Y. A. Sphingolipid metabolism and neutral sphingomyelinases. *Handb. Exp. Pharmacol.* 57–76 (2013).
95. Munk, R. *et al.* Acid ceramidase promotes senescent cell survival. *Aging* **13**, 15750–15769 (2021).
96. Kim, M. K. *et al.* Links between accelerated replicative cellular senescence and down-regulation of SPHK1 transcription. *BMB Rep.* **52**, 220–225 (2019).
97. Venable, M. E., Lee, J. Y., Smyth, M. J., Bielawska, A. & Obeid, L. M. Role of ceramide in cellular senescence. *J. Biol. Chem.* **270**, 30701–30708 (1995).
98. Van Brocklyn, J. R. & Williams, J. B. The control of the balance between ceramide and sphingosine-1-phosphate by sphingosine kinase: oxidative stress and the seesaw of cell survival and death. *Comp. Biochem. Physiol. B Biochem. Mol. Biol.* **163**, 26–36 (2012).
99. Nikolova-Karakashian, M. N. & Rozenova, K. A. Ceramide in stress response. *Adv. Exp. Med. Biol.* **688**, 86–108 (2010).
100. Cuvillier, O. *et al.* Suppression of ceramide-mediated programmed cell death by sphingosine-1-phosphate. *Nature* **381**, 800–803 (1996).
101. Realini, N. *et al.* Acid Ceramidase in Melanoma: EXPRESSION, LOCALIZATION, AND EFFECTS OF PHARMACOLOGICAL INHIBITION. *J. Biol. Chem.* **291**, 2422–2434 (2016).
102. Bizzozero, L. *et al.* Acid sphingomyelinase determines melanoma progression and metastatic behaviour via the microphtalmia-associated transcription factor signalling pathway. *Cell Death Differ.* **21**, 507–520 (2014).
103. Russo, S. B., Ross, J. S. & Cowart, L. A. Sphingolipids in obesity, type 2 diabetes, and metabolic disease. *Handb. Exp. Pharmacol.* 373–401 (2013).

104. Apostolopoulou, M. *et al.* Specific Hepatic Sphingolipids Relate to Insulin Resistance, Oxidative Stress, and Inflammation in Nonalcoholic Steatohepatitis. *Diabetes Care* **41**, 1235–1243 (2018).

105. Luukkonen, P. K. *et al.* Hepatic ceramides dissociate steatosis and insulin resistance in patients with non-alcoholic fatty liver disease. *J. Hepatol.* **64**, 1167–1175 (2016).

106. Turpin, S. M. *et al.* Obesity-induced CerS6-dependent C16:0 ceramide production promotes weight gain and glucose intolerance. *Cell Metab.* **20**, 678–686 (2014).

107. Jiang, X. C. *et al.* Plasma sphingomyelin level as a risk factor for coronary artery disease. *Arterioscler. Thromb. Vasc. Biol.* **20**, 2614–2618 (2000).

108. Havulinna, A. S. *et al.* Circulating Ceramides Predict Cardiovascular Outcomes in the Population-Based FINRISK 2002 Cohort. *Arterioscler. Thromb. Vasc. Biol.* **36**, 2424–2430 (2016).

109. Hadas, Y. *et al.* Altering Sphingolipid Metabolism Attenuates Cell Death and Inflammatory Response After Myocardial Infarction. *Circulation* **141**, 916–930 (2020).

110. Kowalski, G. M., Carey, A. L., Selathurai, A., Kingwell, B. A. & Bruce, C. R. Plasma sphingosine-1-phosphate is elevated in obesity. *PLoS One* **8**, e72449 (2013).

111. Samad, F., Hester, K. D., Yang, G., Hannun, Y. A. & Bielawski, J. Altered adipose and plasma sphingolipid metabolism in obesity: a potential mechanism for cardiovascular and metabolic risk. *Diabetes* **55**, 2579–2587 (2006).

112. Knapp, M. Cardioprotective role of sphingosine-1-phosphate. *J. Physiol. Pharmacol.* **62**, 601–607 (2011).

113. Hughes, J. E. *et al.* Sphingosine-1-phosphate induces an antiinflammatory phenotype in macrophages. *Circ. Res.* **102**, 950–958 (2008).

114. Holland, W. L. *et al.* Receptor-mediated activation of ceramidase activity initiates the

pleiotropic actions of adiponectin. *Nat. Med.* **17**, 55–63 (2011).

115. Pyne, N. J. & Pyne, S. Sphingosine 1-phosphate and cancer. *Nat. Rev. Cancer* **10**, 489–503 (2010).

116. Calle, E. E. & Thun, M. J. Obesity and cancer. *Oncogene* **23**, 6365–6378 (2004).

117. Johnson, E. L. *et al.* Sphingolipids produced by gut bacteria enter host metabolic pathways impacting ceramide levels. *Nat. Commun.* **11**, 2471 (2020).

118. Park, J. C. & Im, S.-H. Of men in mice: the development and application of a humanized gnotobiotic mouse model for microbiome therapeutics. *Exp. Mol. Med.* **52**, 1383–1396 (2020).

119. Stoffel, W., Dittmar, K. & Wilmes, R. Sphingolipid metabolism in Bacteroideaceae. *Hoppe Seylers Z. Physiol. Chem.* **356**, 715–725 (1975).

120. Brown, E. M. *et al.* Bacteroides-Derived Sphingolipids Are Critical for Maintaining Intestinal Homeostasis and Symbiosis. *Cell Host Microbe* **25**, 668–680.e7 (2019).

121. An, D. *et al.* Sphingolipids from a symbiotic microbe regulate homeostasis of host intestinal natural killer T cells. *Cell* **156**, 123–133 (2014).

122. Hildebrand, F. *et al.* Inflammation-associated enterotypes, host genotype, cage and inter-individual effects drive gut microbiota variation in common laboratory mice. *Genome Biol.* **14**, R4 (2013).

123. Wang, J. *et al.* Dietary history contributes to enterotype-like clustering and functional metagenomic content in the intestinal microbiome of wild mice. *Proc. Natl. Acad. Sci. U. S. A.* **111**, E2703–10 (2014).

124. Arthur, J. C. *et al.* Intestinal inflammation targets cancer-inducing activity of the microbiota. *Science* **338**, 120–123 (2012).

125. Walters, W. *et al.* Improved Bacterial 16S rRNA Gene (V4 and V4-5) and Fungal Internal Transcribed Spacer Marker Gene Primers for Microbial Community Surveys. *mSystems* **1**, (2016).

126. Banks, D. E. *et al.* Absence of hyperresponsiveness to methacholine in a worker with methylene diphenyl diisocyanate (MDI)-induced asthma. *Chest* **89**, 389–393 (1986).

127. Zhong, X. *et al.* , the Predominant Bacterium to Predict the Severity of Liver Injury in Alcoholic Liver Disease. *Front. Cell. Infect. Microbiol.* **11**, 649060 (2021).

128. Zagato, E. *et al.* Endogenous murine microbiota member Faecalibaculum rodentium and its human homologue protect from intestinal tumour growth. *Nat Microbiol* **5**, 511–524 (2020).

129. Nie, K. *et al.* : A Beneficial Gut Organism From the Discoveries in Genus and Species. *Front. Cell. Infect. Microbiol.* **11**, 757718 (2021).

130. Molino, S., Lerma-Aguilera, A., Jiménez-Hernández, N., Rufián Henares, J. Á. & Francino, M. P. Evaluation of the Effects of a Short Supplementation With Tannins on the Gut Microbiota of Healthy Subjects. *Front. Microbiol.* **13**, 848611 (2022).

131. Seelan, R. S. *et al.* Human acid ceramidase is overexpressed but not mutated in prostate cancer. *Genes Chromosomes Cancer* **29**, 137–146 (2000).

132. Pitson, S. M. *et al.* Activation of sphingosine kinase 1 by ERK1/2-mediated phosphorylation. *EMBO J.* **22**, 5491–5500 (2003).

133. Saad, A. F. *et al.* The functional effects of acid ceramidase overexpression in prostate cancer progression and resistance to chemotherapy. *Cancer Biol. Ther.* **6**, 1455–1460 (2007).

134. Smith, E. L. & Schuchman, E. H. The unexpected role of acid sphingomyelinase in cell death and the pathophysiology of common diseases. *FASEB J.* **22**, 3419–3431 (2008).

135. Zalatan, J. G., Fenn, T. D., Brunger, A. T. & Herschlag, D. Structural and functional comparisons of nucleotide pyrophosphatase/phosphodiesterase and alkaline phosphatase: implications for mechanism and evolution. *Biochemistry* **45**, 9788–

9803 (2006).

136. Vacca, M. *et al.* The Controversial Role of Human Gut Lachnospiraceae. *Microorganisms* **8**, (2020).

137. Magne, F. *et al.* The Firmicutes/Bacteroidetes Ratio: A Relevant Marker of Gut Dysbiosis in Obese Patients? *Nutrients* **12**, (2020).

138. Zhang, J., Wang, C., Wang, J. & Zhang, F. Relationship between intestinal flora and inflammatory factors in patients with nonalcoholic steatohepatitis. *Exp. Ther. Med.* **15**, 723–726 (2018).

139. Liu, J. *et al.* Comparison of the gut microbe profiles and numbers between patients with liver cirrhosis and healthy individuals. *Curr. Microbiol.* **65**, 7–13 (2012).

140. Cintra, D. E. *et al.* Interleukin-10 is a protective factor against diet-induced insulin resistance in liver. *J. Hepatol.* **48**, 628–637 (2008).

141. Gao, M. *et al.* Hydrodynamic delivery of mIL10 gene protects mice from high-fat diet-induced obesity and glucose intolerance. *Mol. Ther.* **21**, 1852–1861 (2013).

142. van Exel, E. *et al.* Low production capacity of interleukin-10 associates with the metabolic syndrome and type 2 diabetes : the Leiden 85-Plus Study. *Diabetes* **51**, 1088–1092 (2002).

143. Henkes, L. E. *et al.* Acid sphingomyelinase involvement in tumor necrosis factor alpha-regulated vascular and steroid disruption during luteolysis in vivo. *Proc. Natl. Acad. Sci. U. S. A.* **105**, 7670–7675 (2008).

144. Kolesnick, R. & Hannun, Y. A. Ceramide and apoptosis. *Trends Biochem. Sci.* **24**, 224–5; author reply 227 (1999).

145. Jarvis, W. D. *et al.* Induction of apoptotic DNA damage and cell death by activation of the sphingomyelin pathway. *Proc. Natl. Acad. Sci. U. S. A.* **91**, 73–77 (1994).

146. Holland, W. L. *et al.* Inhibition of ceramide synthesis ameliorates glucocorticoid-, saturated-fat-, and obesity-induced insulin resistance. *Cell Metab.* **5**, 167–179

(2007).

147. Ogretmen, B. & Hannun, Y. A. Biologically active sphingolipids in cancer pathogenesis and treatment. *Nat. Rev. Cancer* **4**, 604–616 (2004).

148. Morales, A. *et al.* Pharmacological inhibition or small interfering RNA targeting acid ceramidase sensitizes hepatoma cells to chemotherapy and reduces tumor growth in vivo. *Oncogene* **26**, 905–916 (2007).

149. Papoutsopoulou, S. *et al.* Impact of Interleukin 10 Deficiency on Intestinal Epithelium Responses to Inflammatory Signals. *Front. Immunol.* **12**, 690817 (2021).

150. Wang, P., Wu, P., Siegel, M. I., Egan, R. W. & Billah, M. M. Interleukin (IL)-10 inhibits nuclear factor kappa B (NF kappa B) activation in human monocytes. IL-10 and IL-4 suppress cytokine synthesis by different mechanisms. *J. Biol. Chem.* **270**, 9558–9563 (1995).

151. Mannino, M. H. *et al.* The paradoxical role of IL-10 in immunity and cancer. *Cancer Lett.* **367**, 103–107 (2015).

152. Webster, J. D. & Vucic, D. The Balance of TNF Mediated Pathways Regulates Inflammatory Cell Death Signaling in Healthy and Diseased Tissues. *Front Cell Dev Biol* **8**, 365 (2020).

153. Chen, Q., Daniel, V., Maher, D. W. & Hersey, P. Production of IL-10 by melanoma cells: examination of its role in immunosuppression mediated by melanoma. *Int. J. Cancer* **56**, 755–760 (1994).

154. Itakura, E. *et al.* IL-10 expression by primary tumor cells correlates with melanoma progression from radial to vertical growth phase and development of metastatic competence. *Mod. Pathol.* **24**, 801–809 (2011).

155. York, A. G. *et al.* IL-10 constrains sphingolipid metabolism via fatty acid desaturation to limit inflammation. *bioRxiv* 2023.05.07.539780 (2023) doi:10.1101/2023.05.07.539780.

156. Duan, R.-D. Alkaline sphingomyelinase: an old enzyme with novel implications. *Biochim. Biophys. Acta* **1761**, 281–291 (2006).

157. Kurek, K. *et al.* Metabolism, physiological role, and clinical implications of sphingolipids in gastrointestinal tract. *Biomed Res. Int.* **2013**, 908907 (2013).

158. Li, W. *et al.* Sphingolipids in foodstuff: Compositions, distribution, digestion, metabolism and health effects - A comprehensive review. *Food Res. Int.* **147**, 110566 (2021).

159. Nyberg, L., Duan, R. D., Axelson, J. & Nilsson, A. Identification of an alkaline sphingomyelinase activity in human bile. *Biochim. Biophys. Acta* **1300**, 42–48 (1996).

Supplementary Figures

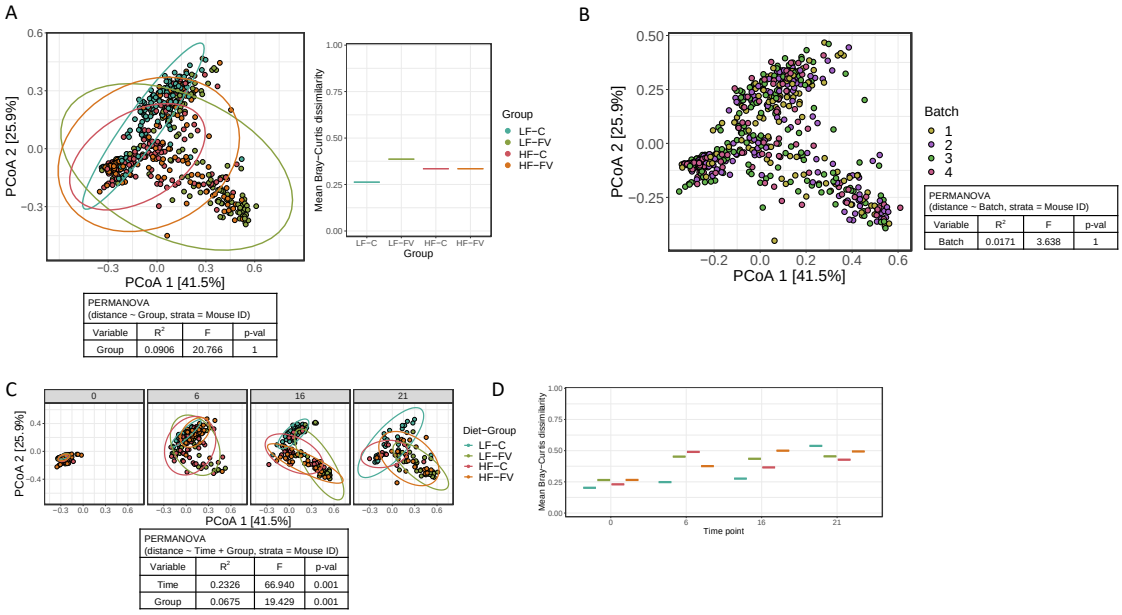

SFig 1: Effect of diet and batch alone on β-diversity.

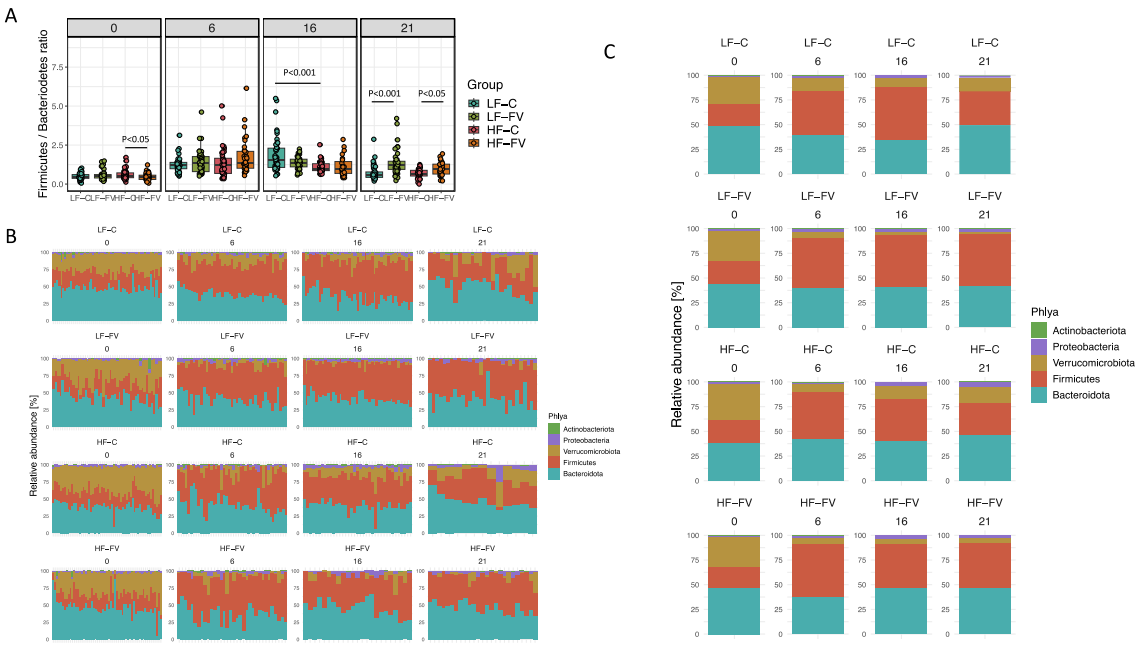

SFig 2: Firmicutes/Bacteroidetes ratio calculated from relative abundance and composition bar plots (phylum level) reveal increased levels of Firmicutes and reduced Verrucomicrobiota with F&V supplementation.

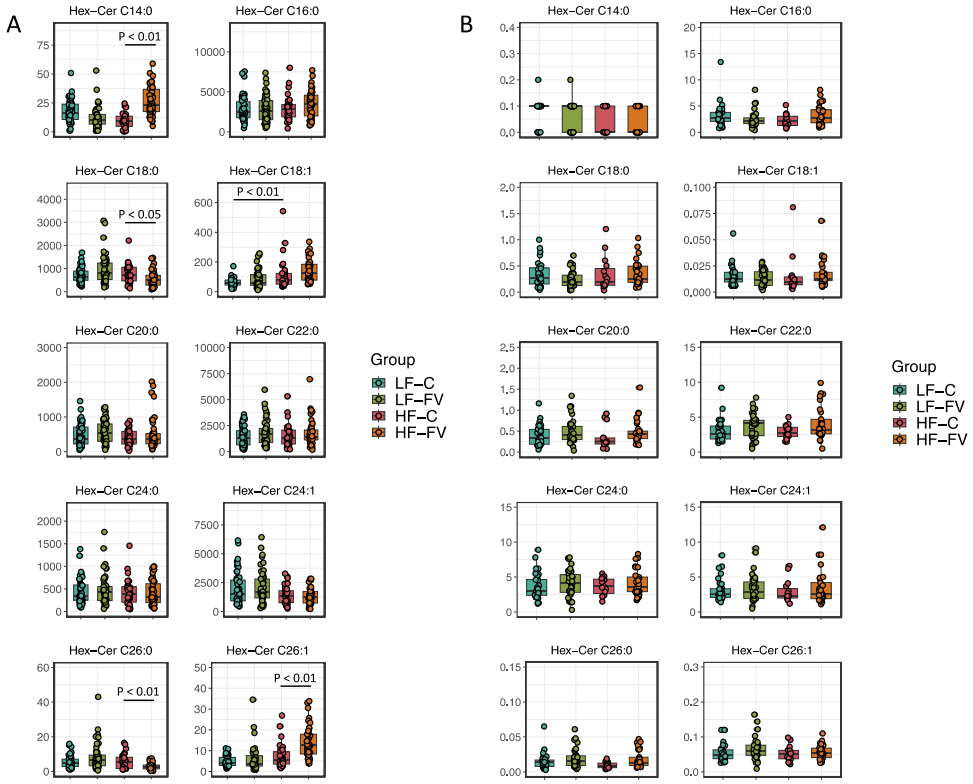

SFig 3: F&V has minor impact on circulating levels of Hex-Cer and no significant differences in liver levels of Hex-Cer.

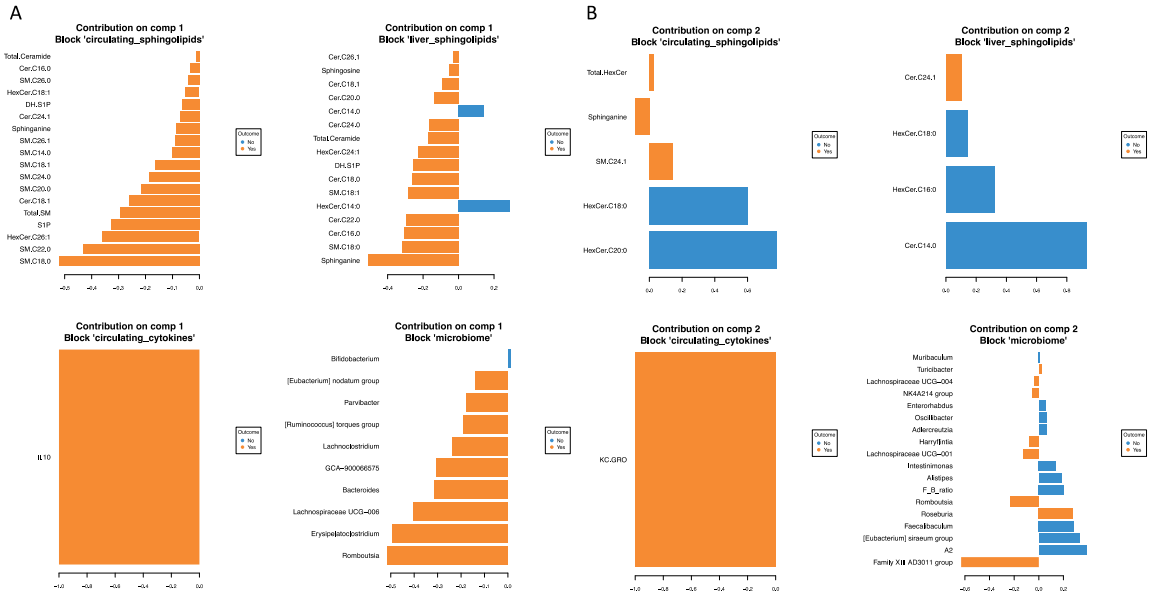

SFig 4: Sparse projection latent structure discriminant analysis selected variables and respective weights for the four blocks in component 1 and 2 that can best discriminate Liver cancer status

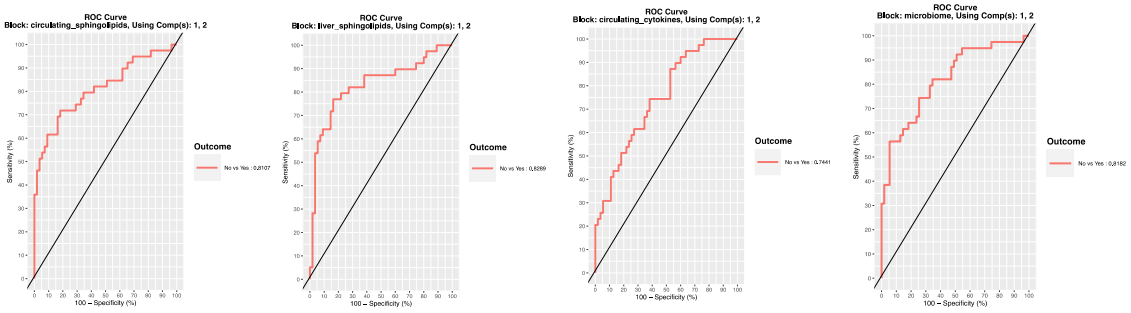

SFig 5: SFig 5: Receiver operating characteristic curves for each ‘omic’ block using component 1 and 2